European Journal of Medicinal Chemistry 218 (2021) 113394

Contents lists available at ScienceDirect

European Journal of Medicinal Chemistry

journal homepage: http://www.elsevier.com/locate/ejmech

Discovery of imidazopyrrolopyridines derivatives as novel and selective inhibitors of JAK2

Pengfei Xu [a], Pei Shen [a], Hai Wang [d], Lian Qin [a], Jie Ren [a], Qiushuang Sun [a], Raoling Ge [c], Jinlei Bian [a, b], Yi Zhong [a, b], Zhiyu Li [a, b, *], JuBo Wang [a, b, ***], Zhixia Qiu [a, b, **]

[a] Department of Medicinal Chemistry, China Pharmaceutical University, 24 Tongjiaxiang, Nanjing, 210009, PR China
[b] Jiangsu Key Laboratory of Drug Design and Optimization, China Pharmaceutical University, Nanjing, 21009, China
[c] Institute of Medical Biology, Chinese Academy of Medical Sciences, Kunming, 650000, China
[d] Changzhou Siyao Pharmaceutical Co. Ltd. No.567, Zhongwu Avenue, Changzhou, Jiangsu, 213018, China

ARTICLE INFO

Article history:
Received 26 January 2021
Received in revised form
15 March 2021
Accepted 15 March 2021
Available online 26 March 2021

Keywords:
Kinase
Janus kinase 2 (JAK2)
Imidazopyrrolopyridine
Myeloproliferative neoplasms
Selectivity

ABSTRACT

Herein, we describe the design, synthesis, and structure–activity relationships of a series of imidazopyrrolopyridines derivatives that selectively inhibit Janus kinase 2 (JAK2). These screening cascades revealed that **6k** was a preferred compound, with IC_{50} values of 10 nM for JAK2. Moreover, **6k** was a selective JAK2 inhibitor with 19-fold, >30-fold and >30-fold selectivity over JAK1, JAK3 and TYK2 respectively. In cytokine-stimulated cell-based assays, **6k** exhibited a higher JAK2 selectivity over JAK1 isoforms. Indeed, at a dose of 20 mg/kg compound **6k**, pSTAT3 and pSTAT5 expression was reduced to levels comparable to those of control animals untreated with GM-CSF. Additionally, **6k** showed a relatively good bioavailability (F = 38%), a suitable half-life time ($T_{1/2}$ = 1.9 h), a satisfactory metabolic stability, suggesting that **6k** might be a promising inhibitor of JAK2 for further development research for the treatment of MPNs.

1. Introduction

Hematologic malignancies which mainly include Leukemia, Lymphoma, Myelodysplastic Syndrome (MDS), and Multiple Myeloma (MM) are a group of diseases caused by disorders of the hematopoietic system [1]. MDS are a group of heterogeneous myeloid clonal diseases that originate from hematopoietic stem cells. They are characterized by abnormal differentiation and development of myeloid cells, manifested as ineffective hematopoiesis, refractory blood cell reduction, and hematopoietic functional failure [2]. Scientists have conducted an in-depth research of the pathogenesis of hematologic malignancies and thus found that certain genetic mutations including mutations in the JAK2 gene lead to signal transduction disorders in different tissues and cells which may resulted in the causing of these diseases [3,4]. Therefore, a variety of kinase inhibitors targeted JAK2 have been developed such as **Ruxolitinib**, **Fedratinib**, **Pacritinib**, and **BMS-911543** based on the pathogenesis of such diseases [5,6].

Janus kinase 2 (JAK2) is an intracellular non-receptor tyrosine kinase that belongs to the JAK family kinases (JAK1, JAK2, JAK3 and TYK2). The JAK-signal transducer and activator of transcription (JAK - STAT) pathway mediates signaling by cytokines, which controls the survival, proliferation and differentiation of a variety of cells [7]. JAK2 phosphorylation, downstream STAT phosphorylation and activation of gene transcription ultimately results in increased proliferation, differentiation, and survival of erythroid and myeloid cells [8]. JAK2 was proven to be critical for the growth and progression of hematologic malignancies especially for myeloproliferative neoplasms among the four JAK subtypes [9]. Currently, a number of pan-JAK and selective JAK inhibitors have been discovered (Fig. 1). JAK1/2 inhibitor **Ruxolitinib** and JAK2/FLT3 inhibitor **Fedratinib** were successively approved by FDA for the treatment of

Abbreviations: JAKs, Janus kinases; JAK2, Janus kinase 2; JAK1, Janus kinase 1; SARs, structure activity relationships; MDS, Myelodysplastic Syndrome; MM, Multiple Myeloma; JAK-STAT, JAK-Signal Transducer and Activator of Transcription; FLT3, Fms-like tyrosine kinase 3; MF, myelofibrosis; MPNs, myeloproliferative neoplasms; DMF *N*, *N*-Dimethylformamide.

* Corresponding author. Department of Medicinal Chemistry, China Pharmaceutical University, 24 Tongjiaxiang, Nanjing, 210009, PR China.
** Corresponding author. Department of Medicinal Chemistry, China Pharmaceutical University, 24 Tongjiaxiang, Nanjing, 210009, PR China.
*** Corresponding author. Department of Medicinal Chemistry, China Pharmaceutical University, 24 Tongjiaxiang, Nanjing, 210009, PR China.
E-mail address: zhiyuli@cpu.edu.cn (Z. Li).

https://doi.org/10.1016/j.ejmech.2021.113394
0223-5234/

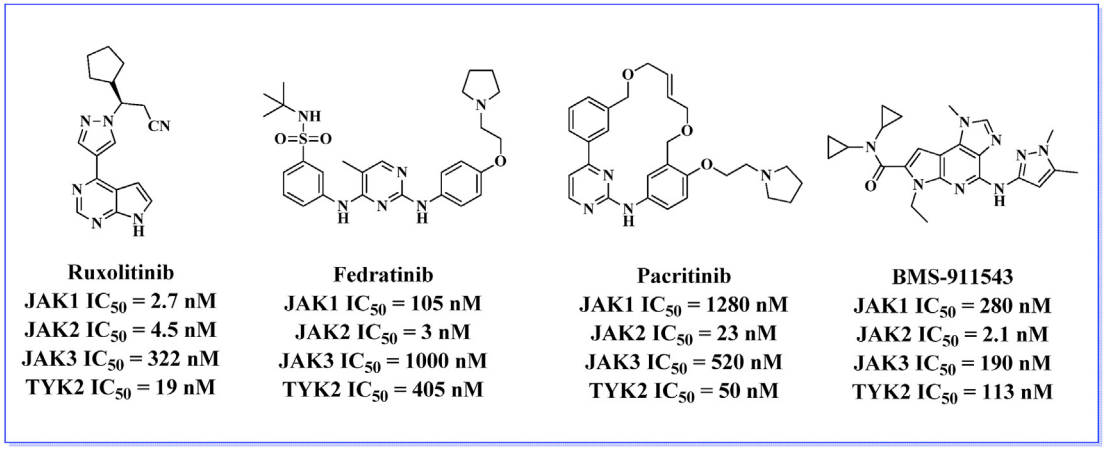

Fig. 1. Structures of representative JAK2 inhibitors.

myelofibrosis (MF) and polycythemia vera [10,11]. Another JAK2 inhibitor, **BMS-911543**, is currently in phase II clinical tial [12].

The approval of the JAK2 inhibitors **Ruxolitinib** and **Fedratinib** for the treatment of myeloproliferative neoplasms (MPNs) reinforced the feasibility of targeting the JAK family specifically. However, the high level of sequence conservation in the kinase domains of the JAK family is a key challenge for the design of selective JAK2 inhibitors [13]. Our recent research work discovered the compound **1a**, an imidazopyrrolopyridines derivative, as a potent selective JAK2 inhibitor with IC_{50} for JAK1 and JAK2 are >400 nM and 19 nM respectively but less potent in cellular activity. We supposed that the poor cell activity was due to the high polarity of this molecule. In addition, the overall molecular weight of this compound is relatively high which led to low ligand efficiency. As a result, we explored the compound groups that affect the activity of JAK2 kinase in detail to obtain these imidazopyrrolopyridines analogues as potent JAK2 inhibitors in this work.

2. Results and discussion

2.1. Design and biochemical activity

Based on the structure comparison between the approved JAK inhibitor **Baricitinib** and a reported JAK inhibitor **Compound 31**, we designed a novel series of JAK inhibitors as shown in Fig. 2. **Compound 31** has excellent biological activities against JAKs, both in vitro and in vivo [14]. Meanwhile, **Baricitinib** is a highly potent JAK2 inhibitor. According to the combination principle of structural fragments, we designed imidazopyrrolopyridines derivative **1a** which exhibited highly and excellent biological activity against JAK2. Besides, docking study revealed that the furimethylene hydroxy could form hydrogen bonding with Asp939 in JAK2 while there was no interaction for the group of 1-(ethylsulfonyl)azetidine acetonitrile. Additionally, structure–activity relationship (SAR) studies showed that the removal of 1-(ethylsulfonyl)azetidine in these analogues did not influence their JAK inhibition significantly. As a result, a series of 1-(1H-pyrazol-4-yl)- imidazopyrrolopyridines derivatives were synthesized to explore the SAR between groups and the biological activities for JAK2.

The imidazopyrrolopyridines derivatives were screened for their in vitro kinase inhibitory activities toward JAK1 and JAK2 for IC_{50} or inhibition at 30 nM. **Baricitinib** (an approved JAK inhibitor; IC_{50} for JAK1 and JAK2 were 4.0 nM and 6.6 nM respectively) were used as positive controls [15]. All the inhibition or IC_{50} results were shown in Table 1–3. SAR studies began with variation of the imidazole C-2 group or the removal of the cyanoethyl as shown in Table 1. The modification of R_1 group such as methylthiophene, thiophene or methylfuran did not influence their JAK2 inhibition and JAK1 selectivity significantly. At the same time, the extension of terminal alkyl chain resulted in compounds **2a** and **3a** reduced their JAK2 inhibition slightly. Compound **1a** was docked into the ATP binding pocket of JAK2 using MOE 2020.01 in order to investigate the binding mode of it in JAK2 (Fig. 3, **A**) [16]. The result shown in Fig. 3 suggested that the –NH and = N moieties of azaindole in compound **1a** could form hydrogen bonds with GLU930 and LEU932. These hydrogen interactions were the crucial part for the protein kinase inhibition. There seemed to be no interaction between the cyanoethyl and the JAK2 kinase from this docking results. As a result, the next step of modifications focused on the removal of the cyanoethyl to simplify molecules of these analogues. However, deletion of the cyanoethyl lead to reduced JAK2 inhibition significantly such as compound **2c**, **3c** and **4c**. The bring back of the cyanoethyl resulted in the restoration of JAK2 activity indicated that the cyano group on pyrazole ring contributed much more to JAK2 inhibition that needed to be maintained.

After confirming the importance of the cyano group, these derivatives were simplified through the deletion of the part of azetidine and the compound **5a** was synthesized with IC_{50} (43 nM) for JAK2. When the propionitrile was replaced by acetonitrile to afford the compound **6a**, the kinase inhibition activity was further reduced which indicated that a suitable length of side chain connecting cyano was favorable for the activity against JAK2 kinase. Propionitrile was preserved and different R_1 substituted groups were explored during our initial screen. Results in Table 2 showed that compounds **5b-5k** exhibited moderate inhibitory activities against JAK2 except for compound **5e** with the IC_{50} (151 nM), **5f** with the IC_{50} (61 nM) and **5g** with the IC_{50} (65 nM) against JAK2. To further simplify the structure of the molecules, the R_1 groups were removed totally which delivered the compound **5k**. This molecule (M. W = 277.28) gained remarkable inhibition activity against JAK2 (IC_{50} = 15 nM) although the selectivity against JAK1 (IC_{50} = 94 nM) was reduced to some extent. Replaced propionitrile by butylcyanide afforded the compound **6k** and the inhibition activity against JAK2 was further improved. However, when the length of this sidechain was extended or substituted by trifluoromethyl such as compound **7k** and **8k**, the inhibitory activity of JAK2 kinase decreased immediately which indicated that butylcyanide was the most suitable sidechain of these analogues.

5k and **6k** was docked into the ATP binding pocket of JAK2 in order to investigate the binding mode of them in JAK2 (Fig. 3, **B**).

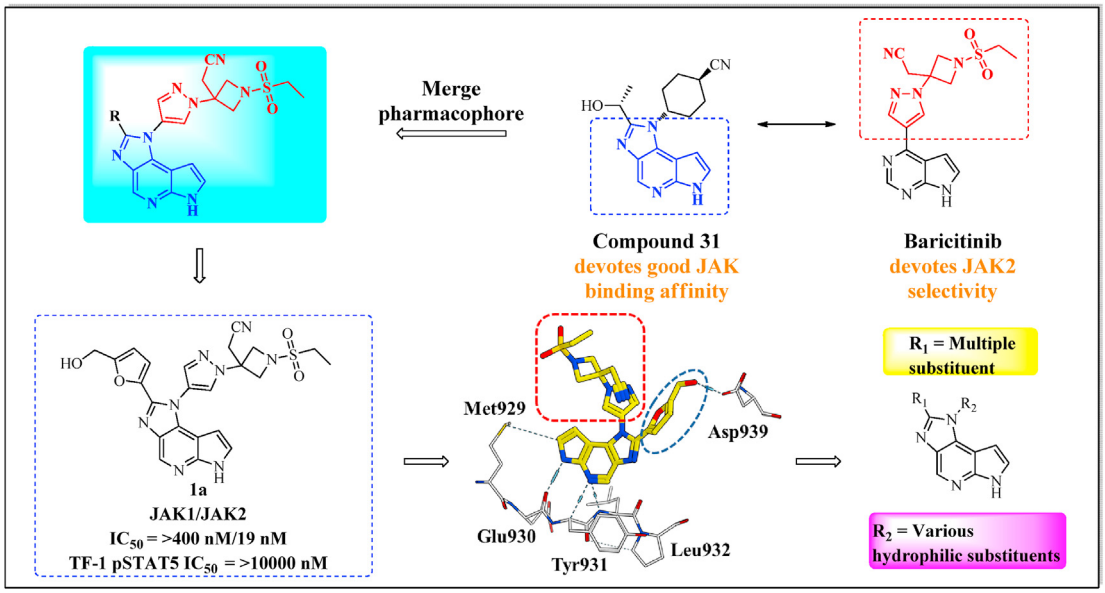

Fig. 2. Design strategy for the target compounds.

The results suggested that the −NH and = N moieties of azaindole in compound **5k** and **6k** could form hydrogen bonds with GLU930 and LEU932 which were the crucial part for the protein kinase inhibition. Additionally, the cyano group of these two compounds form additional hydrogen bonds with LYS882 that could explain the observed good inhibition activity for JAK2 kinase of these compounds. At the same time, the most potent compound **6k** was docked into the ATP binding pocket of JAK1 in order to investigate the reason for its poor JAK1 inhibition. The result exhibited in Fig. 3, **C** indicated that there was no interaction between the cyano group and the amino acid residues of JAK1 kinase which may contribute to low JAK1 inhibition of this compound. Besides, **5d** and **5h** were docked into the ATP binding pocket of JAK2 to explore influences of the R_1 substituted groups. As showed in Fig. 3, **D**, no matter whether there are substituents such as thienyl or methyl thienyl or no substituents, there was no additional interaction forced between compounds and the kinase. Generally, different substituents on the C-2 of the imidazole ring were well tolerated.

Due to the lack of relatively potent selectivity over JAK1 kinase for the compound **6k**, more modifications were applied in these derivatives which were displayed in Table 3. The sidechain of butylcyanide was preserved and heterocyclic aryl such as methyl furan, aminothiazole and methylthiophene along with alicyclic groups such as cyclopropyl, cyclobutyl and cyclopentyl were applied in the R_1 group to improve the selectivity of compounds to JAK1 kinase. From the data shown in Table 3, we could see that this series of derivatives such as compound **6b**, **6d**, **9a**, **9b** and **9c** maintained the inhibitory activity against JAK2 kinase basically and the selectivity to JAK1 kinase was increased. Among them, compound **6d** performed best with the IC_{50} 12 nM for JAK2 and 254 nM for JAK1 (JAK1/JAK2 selectivity>20 folds).

2.2. Chemistry

Compound **1a-d**, **2-3a**, **1e** were synthesized as described in Scheme 1. Generally, the reaction of tert-butyl-3-oxoazetidine-1-carboxylate with 2-diethoxyphosphorylacetonitrile under basic (NaH) condition led to the intermediate tert-butyl-3-(cyanomethylene) azetidine-1-carboxylate, which was then reacted with 4-nitropyrazole using DBU as a catalyst and then reduced under the condition of hydrogen palladium carbon to give target intermediate molecule **11** [17]. Intermediate **13** was obtained from reaction of 4-chloro-7-azaindole with benzenesulfonyl chloride under basic condition of TEA. Then, the key intermediate molecule **14** was afforded through nitration reaction under the condition of tetramethylammonium nitrate and TFAA [18]. The key intermediate **14** reacted with and **11** using K_2CO_3 as a basic at high temperature to produce molecule **15**, which then reduced under the condition of hydrogen palladium carbon to deliver intermediate **16**. Finally, target compounds **1a-d**, **2-3a**, **1e** were yielded through the rection with various aromatic aldehyde, deprotection of the Boc group, sulfonylation with different sulfonyl chloride and Bs-deprotection [19].

Synthetic routes of the other three series of compounds were exhibited in Scheme 2. 4-nitropyrazole was applied for the starting material through the reduction and substitution reaction afforded the key intermediate **19**. Compound **2c** was obtained by reduction of intermediate **19**, cyclization with 2-thenaldehyde, substitution with 1-Boc-3-Iodoazetidine, Boc removal, sulfonylation with trifluoromethanesulfonyl chloride and deprotection of the benzenesulfonyl [20]. The synthetic route of derivatives **3-4c** were similar to that of compound **2c** through reduction, cyclization, substitution, *N*-alkylation and Bs-deprotection reaction to deliver target molecules **3c** and **4c**. The synthesis routes of the largest part of the compounds including **5-6a**, **5b-k**, **6-8k**, **6-7b**, **6-8d** and **9a-d** was similar to the synthesis of derivatives **3-4c**. This series of derivatives were obtained via reaction with virous aldehyde under the condition of $Na_2S_2O_5$ and DMF at 90 °C then with kinds of cyanogen halide and Bs-deprotection through the starting material intermediate **20** [13].

2.3. Biological evaluation

2.3.1. ADME and physicochemical properties of inhibitors

Compounds **1a**, **1c**, **5h**, **6k**, **6b**, **6d** and **9c** were selected for further profiling on the basis of kinase potency and structural diversity considerations. Firstly, log $D_{7.2}$ were measured for these molecules and the results were displayed in Table 4 [21]. This series of analogues along with **Baricitinib** exhibited a reasonable log of distribution coefficient which ranged from 0.24 to 2.42. In our

Table 1
Structures and in vitro biological activities of compounds **1a-1e**, **2a-3a**, **2c-4c**.[a]..

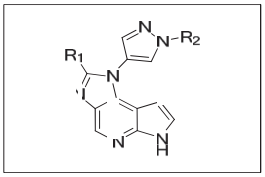

Compd	R_1	R_2	JAK2 IC_{50} or (Inhibition%/30 nM)	JAK1 IC_{50} or (Inhibition%/30 nM)
1a	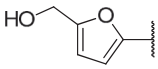	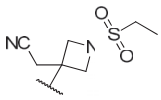	19 nM	>400 nM
1b	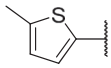	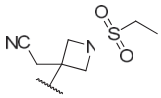	27 nM	246 nM
1c		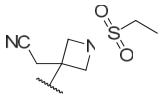	19 nM	>300 nM
1d	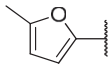	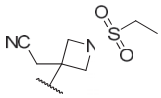	37 nM	>400 nM
2a	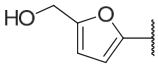	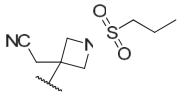	34 nM	n.d.
3a	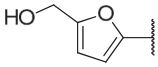	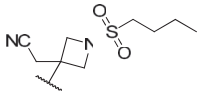	30 nM	n.d.
2c		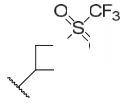	25.1%	24.1%
3c		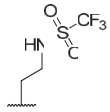	6.5%	4.3%
4c		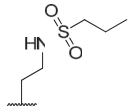	3.2%	n.d.
1e	H	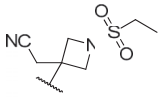	65.8%	n.d.

[a] IC_{50} values or inhibition rates % are a mean of two individual determinations.
[b] n.d. = value not determined.

Table 2
Structures and in vitro biological activities of compounds **5a-5k**, **6a**, **6k-8k**.[a]..

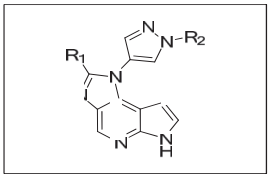

Compd	R_1	R_2	JAK2 IC_{50} or (Inhibition%/30 nM)	JAK1 IC_{50} or (Inhibition%/30 nM)
5a	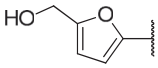	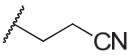	43 nM	>400 nM
6a	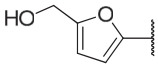	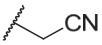	267 nM	n.d.
5b	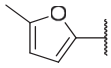	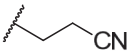	26 nM	>400 nM
5c	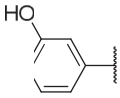	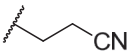	26 nM	n.d.
5d	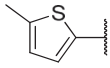	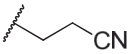	28 nM	9.6%
5e	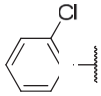	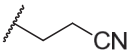	151 nM	n.d.
5f	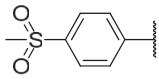	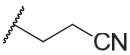	61 nM	n.d.
5g		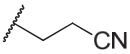	65 nM	>300 nM
5h		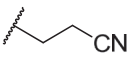	17 nM	254 nM

(*continued on next page*)

Table 2 (*continued*)

Compd	R_1	R_2	JAK2 IC_{50} or (Inhibition%/30 nM)	JAK1 IC_{50} or (Inhibition%/30 nM)
5i		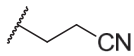	39.5%	n.d.
5j		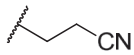	36.6%	n.d.
5k	H	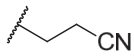	15 nM	94 nM
6k	H	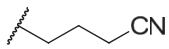	10 nM	185 nM
7k	H	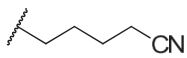	45.9%	n.d.
8k	H	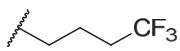	53 nM	154 nM

[a] IC_{50} values or inhibition rates % are a mean of two individual determinations.
[b] n.d. = value not determined.

initial screen process, compound **1a** possessed weak cytokine signaling cellular activity with the IC_{50} (>10 μM) for JAK2 in TF1 cell despite its excellent kinase inhibition activity. Too large tPSA calculated by Chemdraw may be the cause of its poor cell viability and this value had been reduced in a reasonable range after our structural optimization. The solubility of these preferred compounds in aqueous buffer were also determined and most molecules displayed a comparable result with the FDA approved JAKs inhibitor **Baricitinib** especially compound **6k** which possessed 12 times the water solubility of **Baricitinib**. We also tested these compounds in rat liver microsomes to assess the propensity of the template toward degradation by phase I metabolism [22]. In rat liver microsomes, most molecules had a rapid clearance such as compound **1c**, **6b** and **6d** with a half-life of 27.72 min (apparent clearance of 45 mL/min/kg), 30.8 min (apparent clearance of 40.5 mL/min/kg) and 18.0 min (apparent clearance of 69.3 mL/min/kg). Gratifyingly, compound **6k** displayed a superior rat liver microsomes stability with a half-life of 433.13 min (apparent clearance of 2.88 mL/min/kg) which was compared favorably with **Baricitinib**.

2.3.2. Cellular activity

The cellular potency and selectivity of these preferred compounds for each individual kinase were characterized in a series of cytokine-stimulated cell-based assays because of the complexity of the cooperative property of JAK kinases. For instance, IL-4-induced STAT6 phosphorylation is mediated by JAK1 and JAK3 and GM-CSF-induced STAT5 phosphorylation is dependent on JAK2 [23]. As shown in Table 5, to assess JAK2 and JAK1-JAK3 signaling, we stimulated TF-1 and THP-1 cells via GM-CSF and IL-4 and measured the levels of phosphorylated STAT5 and STAT6. In these systems, compound **6k** inhibited the phosphorylation of STAT5 in JAK2 signaling with an IC_{50} value of 269 nM and the phosphorylation of STAT6 in JAK1-JAK3 signaling with an IC_{50} value of 10.69 μM. The data from these in vitro enzyme and cell-based assays indicated that **6k** inhibited JAK2 rather than JAK1 or JAK3.

In order to verify the mechanism of compound **6k** in the JAK2-STAT signaling pathway, the phosphorylation levels of JAK2's downstream substrate was evaluated. As shown in Fig. 4, the treatment of the TF1 cells with compound **6k** or **Baricitinib** led to the decrease of pSTAT5 (Y694) level. The pSTAT5 signal intensities decreased sharply at 0.3 μM in TF1 cells and also downregulated pSTAT5 in a dose-dependent manner from 0.3 to 10 μM. Overall, these results revealed that compound **6k** down-regulated the JAK2-STAT signaling pathway by inhibiting JAK2 kinase activity in TF1 cells.

2.3.3. In vivo pharmacokinetics

Compounds **6k** with potent JAK2 inhibitory activity and good JAK1, JAK3 and TYK2 selectivity as well as promising cellular potency was selected for further evaluation, and plasma concentration was determined after oral (PO, 20 mg/kg) and intravenous (IV, 5 mg/kg) administration in rats (Table 6) together with **Baricitinib**. Compound **6k** presented a moderate PK profile in rats, high

Table 3
Structures and in vitro biological activities of compounds **6b-7b**, **6d-8d**, **9a-9d**.[a]..

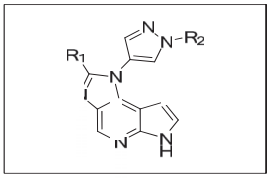

Compd	R_1	R_2	JAK2 IC_{50} or (Inhibition%/30 nM)	JAK1 IC_{50} or (Inhibition%/30 nM)
6b	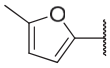	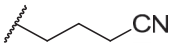	14 nM	12.6%
7b	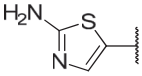	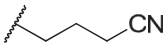	29.7%	n.d.
6d	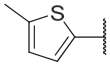	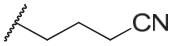	12 nM	251 nM
7d	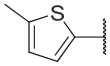	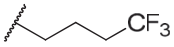	21.5%	n.d.
8d	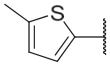	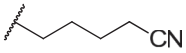	37.8%	n.d.
9a		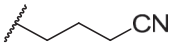	51.4%	n.d.
9b		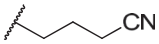	61.8%	n.d.
9c		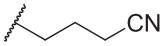	18 nM	15.2%
9d		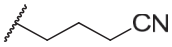	22.3%	n.d.

[a] IC_{50} values or inhibition rates % are a mean of two individual determinations.
[b] n.d. = value not determined.

maximum concentration (C_{max} = 885.62 μg/L) and good plasma duration (MRT = 2.10 h), leading to a high plasma exposure (AUC = 1507.67 μg*h/L) after oral administration. Assessment of pharmacokinetic (PK) properties for compound **6k** in rats also showed good oral bioavailability (F = 38%) and the low clearance and high volume of distribution (38.33 L/kg) led to a suitable half-life of 1.9 h. In general, compound **6k** exhibited a comparable pharmacokinetic property to **Baricitinib**. Thus, compound **6k** could be selected for further evaluation in an in vivo experiment.

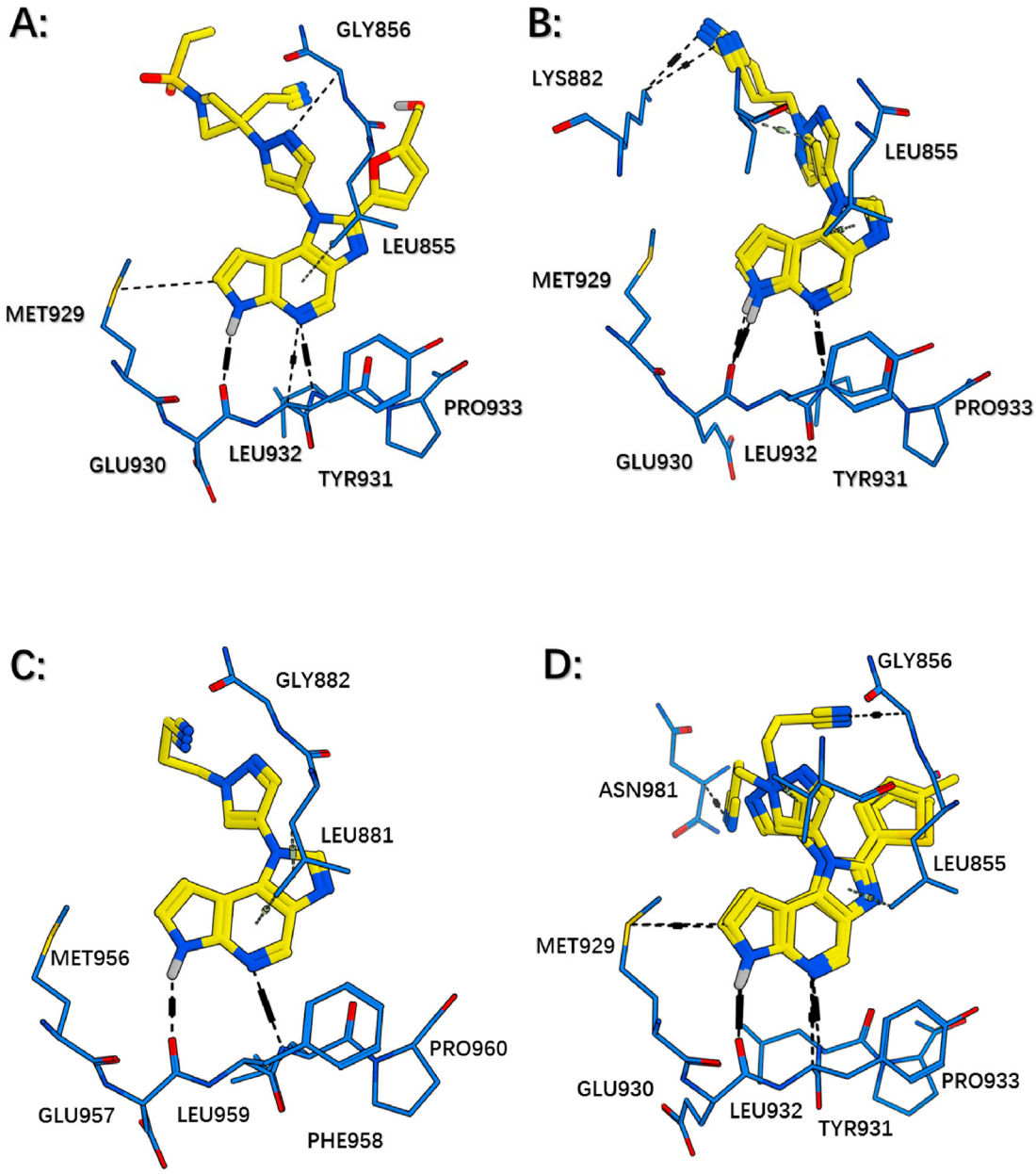

Fig. 3. Docking of compound **1a** with JAK2 (A: PDB code 2XA4). Docking of compound **5k** and **6k** with JAK2 (B: PDB code 2XA4). Docking of compound **6k** with JAK1 (C: PDB code 4IVB). Docking of compound **5d** and **5h** with JAK2 (D: PDB code 2XA4).

2.3.4. In vivo pharmacodynamics

To further assess the biological activity of compound **6k**, its ability to inhibit JAK2-mediated cytokine signaling was evaluated in vivo in a PD experiment in the mouse. As shown in Fig. 5, mice were pretreated with ascending oral doses of compound **6k** ranging from 3 to 50 mg/kg, followed by a 1 μg intraperitoneal (IP) injection of GM-CSF cytokine 30 min later. An additional 30 min after GM-CSF administration, concentrations of pSTAT3 and pSTAT5 were measured in snapfrozen spleens. As further demonstrated in Fig. 5, the decreasing pSTAT3 and pSTAT5 levels in the spleens of GM-CSF treated animals were achieved with ascending oral doses of compound **6k** in the mouse. Indeed, at a dose of 20 mg/kg compound **6k**, pSTAT3 and pSTAT5 expression was reduced to levels comparable to those of control animals untreated with GM-CSF, indicating that robust in vivo suppression of JAK2-mediated signaling was achieved.

3. Conclusions

In conclusion, we discovered compound **1a** as a promising lead for a small molecule targeting JAK2 kinase aimed at increasing cellular activity via pharmacophore merge strategy. SAR developed around the designed cycle moieties combined with structure-based design led to the discovery of **6k**, which possessed >18-fold selectivity over JAK1,3, TYK2 in enzyme assays. At the same time, the cell pathway inhibitory activity of the compound **6k** has been greatly improved due to the decrease in tPSA. Additionally, the excellent potency and oral PK properties of **6k** in rats enabled its use in multiple in vivo models for the evaluation of modulating JAK2 driven pharmacodynamic responses. To summarize, compound **6k** is a promising inhibitor of JAK2 for further development research for the treatment of MPNs.

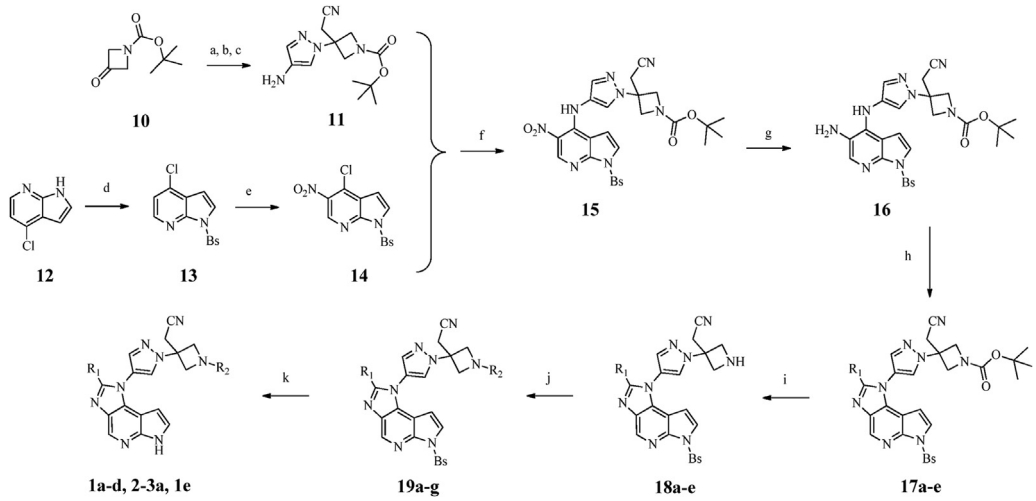

Scheme 1. Synthesis of JAK2 inhibitors. Reagents and conditions: (a) 2-Diethoxyphosphorylacetonitrile, NaH, 0 °C, THF; (b) 4-Nitropyrazole, DBU, 20 °C, MeCN; (c) H_2, Pd/C 20 °C, MeOH; (d) Benzenesulfonyl chloride, TEA, 0 °C, DCM; (e) Tetramethylammonium nitrate, trifluoroacetic anhydride, 20 °C, DCM; (f) K_2CO_3, reflux, THF; (g) H_2, Pd/C 20 °C, MeOH; (h) aldehyde, $Na_2S_2O_5$, 90 °C, DMF or $(EtO)_3CH$, p-TsOH (cat.), reflux, PhMe; (i) CF_3COOH, 30 °C, DCM; (j) Corresponding sulfonyl chloride, K_2CO_3, reflux, THF; (k) NaOH solution, 20 °C, THF/MeOH. Bs = Benzenesulfonyl.

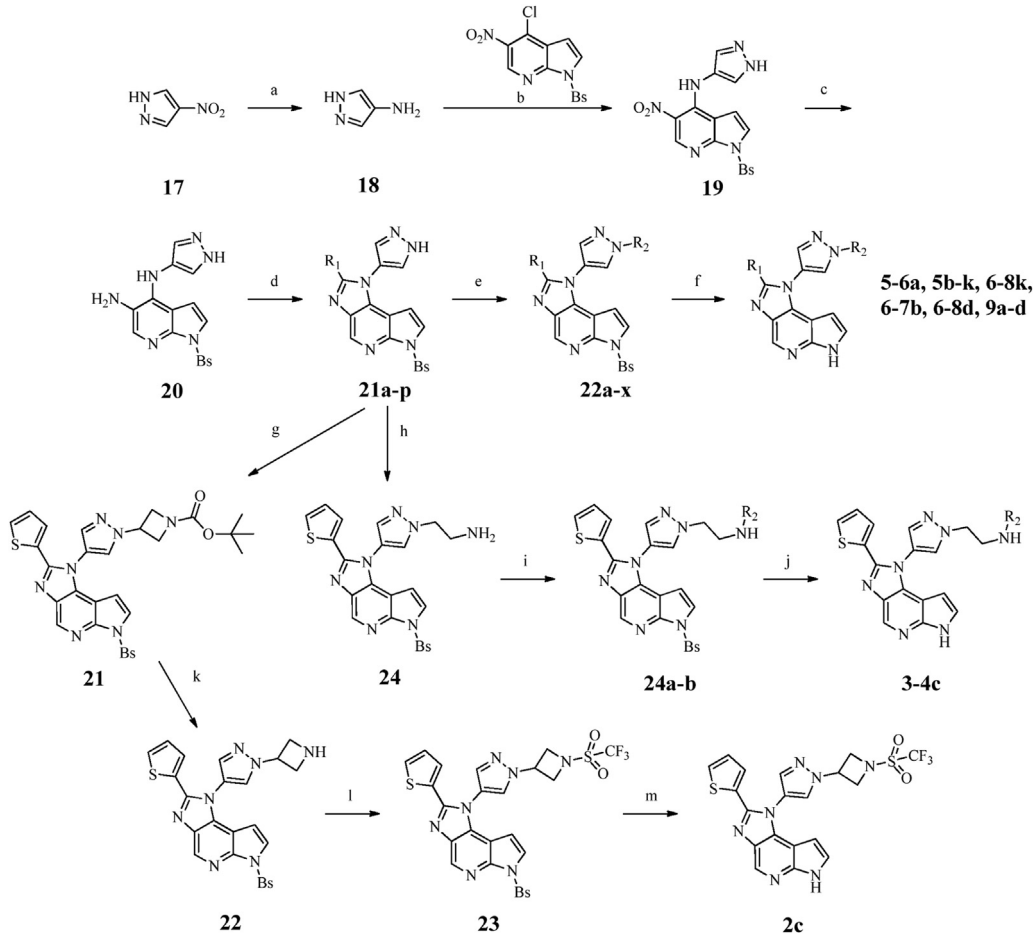

Scheme 2. Synthesis of JAK2 inhibitors. Reagents and conditions: (a) H_2, Pd/C 20 °C, MeOH; (b) K_2CO_3, reflux, THF; (c) H_2, Pd/C 20 °C, MeOH; (d) aldehyde, $Na_2S_2O_5$, 90 °C, DMF or $(EtO)_3CH$, *p*-TsOH (cat.), reflux, PhMe; (e) Corresponding Bromide, K_2CO_3, 80 °C, DMF; (f) NaOH solution, 20 °C, THF/MeOH; (g) 1-Boc-3-Iodoazetidine, K_2CO_3, 90 °C, DMF; (h) 2-Bromoethylamine Hydrobromide, NaH, 25 °C, DMF; (i) Corresponding sulfonyl chloride, K_2CO_3, reflux, THF; (j) NaOH solution, 20 °C, THF/MeOH; (k) CF_3COOH, 30 °C, DCM; (l) Trifluoromethanesulfonyl chloride, DIPEA, 20 °C, THF; (m) NaOH solution, 20 °C, THF/MeOH. Bs = Benzenesulfonyl.

Table 4
Physicochemical properties and metabolic stability of preferred compounds.

Compd	log $D_{7.2}$[a]	tPSA[b]	Aqueous solubility (ug/mL)[c]	CL (mL/min/kg)[d]	$T_{1/2}$ (min)[d]	Stability (%) (2h)[d]
1a	0.95	146.22	5.19	n.d.[e]	n.d.	n.d.
1c	1.95	116.76	9.98	45	27.72	3.43
5h	1.98	79.38	23.13	29.34	42.52	13.02
6k	0.81	79.38	194.36	2.88	433.13	80.83
6b	2.09	88.61	34.29	40.5	30.8	5.85
6d	2.42	79.38	1.31	69.3	18.0	0.94
9c	1.63	79.38	77.03	25.74	48.46	17.99
Baricitinib	0.24	113.52	16.3	/	/	96.12

[a] Measured log of distribution coefficient between octanol and aqueous pH 7.2 buffer.
[b] Topological polar surface area predicted by Chemdraw 12.0.
[c] Solubility of solid powder in aqueous buffer determined by HPLC.
[d] In vitro stability in cryopreserved rat liver microsome.
[e] n. d. = value not determined.

Table 5
In vitro profiles of preferred compounds.[a].

Compd	Enzymes IC_{50} (nM) or (Inhibition%/30 nM)				Cytokine signaling IC_{50} (μM) in THP-1 or TF1 cells	
	JAK1	JAK2	JAK3	TYK2	IL-4 JAK1/JAK3	GM-CSF JAK2/JAK2
1a	>400	19	n.d.[b]	n.d.	>10	>10
1c	>300	19	n.d.	n.d.	>10	0.696
5h	254	17	160	>300	>10	0.306
6k	185	10	>300	>300	10.69	0.269
6b	12.6%	14	n.d.	n.d.	9.56	0.397
6d	251	12	280	>300	5.43	0.321
9c	15.2%	18	n.d.	n.d.	5.33	0.494
Baricitinib	4	7	787	61	0.562	0.470

[a] IC_{50} values or inhibition rates % are a mean of two individual determinations.
[b] n.d. = value not determined.

Table 6
Rat pharmacokinetic profile of compound 6k and baricitinib.[a].

	Compound 6k		Baricitinib	
	dose (mg/kg)			
	5 (IV)	20 (PO)	1 (IV)	5 (PO)
T_{max} (h)	/	0.42	/	1.00
C_{max} (μg/L)	/	885.62	/	659.15
AUC (μg*h/L)	1004.64	1507.67	1586.81	3608.48
CL (L/h/kg)	5.08	14.61	0.63	1.39
V_{ss} (L/kg)	10.10	38.33	1.80	4.88
$T_{1/2}$ (h)	1.46	1.90	1.96	2.43
MRT (h)	0.69	2.10	1.34	4.36
F (%)	/	37.52	/	45.48

[a] IV vehicle: 70/20/10 Normal Saline/PEG400/DMSO. PO vehicle: 70/20/10 Normal Saline/PEG400/DMSO; Three animals were used in each of the control and dosing arms.

4. Experimental

4.1. Chemistry and chemical methods

Chemical Methods. All reagents and solvents purchased from commercial suppliers were used without further purification. ^{1}H NMR spectra were collected on a Bruker AVANCE 300 MHz spectrometer. Chemical shifts (δ) are reported in parts per million (ppm) from tetramethylsilane (TMS) using the residual solvent resonance. Multiplicities are abbreviated as s (singlet), d (doublet), t (triplet), q (quartet), m (multiplet), and br s (broad singlet). HR-MS was recorded on Agilent technologies 6520 Accurate-Mass LC/MS Q-TOF instruments. The procedures outlined in this section are those employed for the reactions run at the largest scale. HPLC analysis was carried out on an Agilent 1260 infinity eluded with isocratic eluting mixed by solvent A (acetonitrile) and solvent B (methanol) at a flow rate of 1 mL/min and at λ = 254 nm.

General synthetic procedure 1: substituted imidazole formation

A solution of **16** or **20** (1.0 equiv) and $Na_2S_2O_5$ (5.0 equiv) in DMF were added aromatic aldehyde (2.0 equiv). The reaction was heated in an open single neck bottle at 90 °C for 12 h, cooled to room temperature, then water was added and aqueous phase was extracted twice with DCM. The combined extracts were washed with brine, dried with sodium sulfate and concentrated under vacuum give the crude product, which was further purified by silica gel column chromatography (ethyl acetate: petroleum ether = 1: 1) to give target product as a brown solid.

General synthetic procedure 2: imidazole formation without substituted groups

A mixture of **16** or **20** (1.0 equiv), triethyl orthoformate (2.5 equiv), and *p*-toluenesulfonic acid monohydrate (0.1 equiv) in toluene (20 mL) was heated at reflux at 24 h. After cooling, ethyl acetate was added and the mixture washed with saturated sodium hydrogen carbonate solution, water and brine, dried with sodium

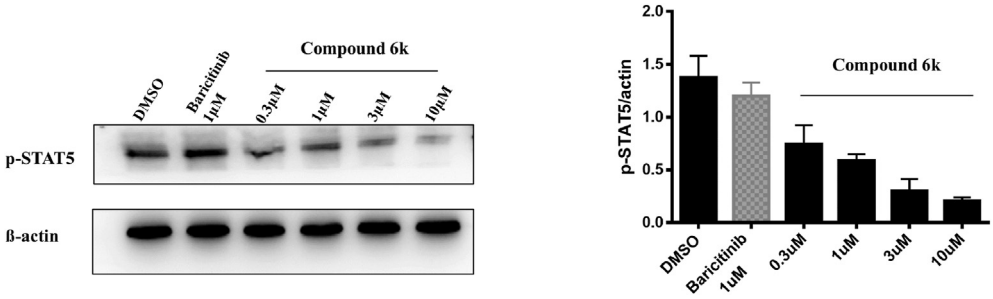

Fig. 4. Western blot analysis of the effects of **Baricitinib** and compound **6k** on the phosphorylation of STAT5 in TF1 cells.

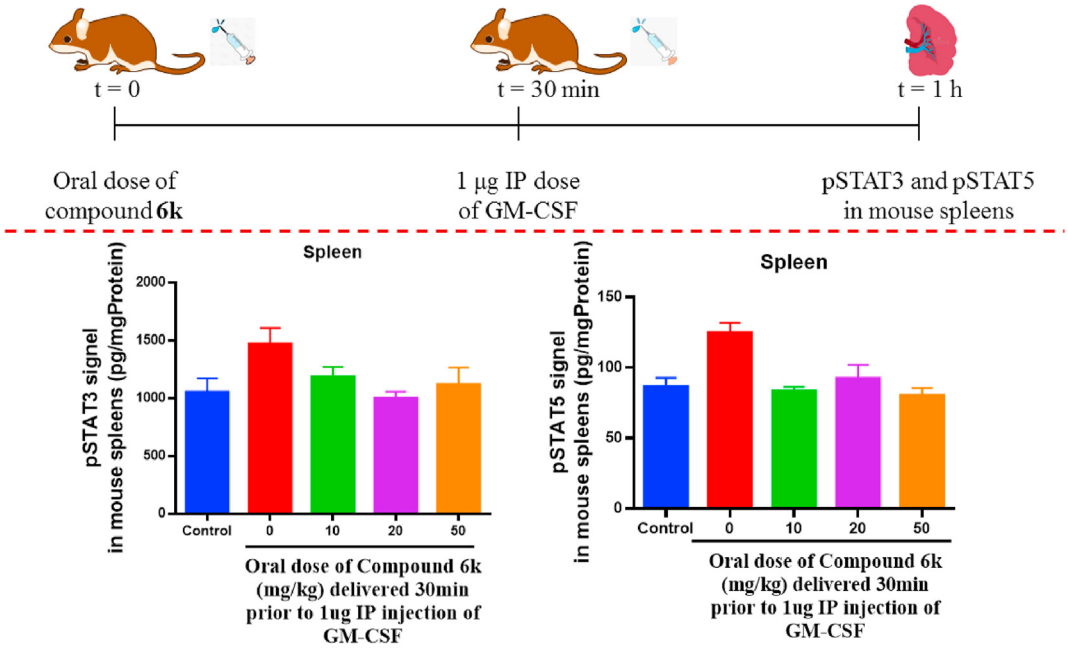

Fig. 5. Design and results of an GM-CSF induced pSTAT3 and pSTAT5 PD study of compound **6k** in the mouse; Measured 30 min after dosing of GM-CSF; Four animals were used in each of the control and dosing arms.

sulfate, and concentrated under vacuum. Purification by silica gel column chromatography afforded target product as a light white solid.

General synthetic procedure 3: TFA-Mediated Boc removal

Boc-protected amine (1.0 equiv) was dissolved in a mixture of TFA (10.0 equiv)/DCM (1:1), and stirred at room temperature for 12 h. The mixture was concentrated under reduced pressure, triturated with diethyl ether, and filtered to give the desired product, which was directly used in the next step without further purification.

General synthetic procedure 4: sulfamide formation

A solution of sulfonyl chloride (1.5 equiv) in THF was added to the solution of heterocyclic secondary amine (1.0 equiv) and potassium carbonate (5.0 equiv). The reaction mixture was heated to reflux for 4 h. The completion of the reaction was checked with TLC. After cooling to room temperature, water was added and aqueous phase was extracted twice with DCM. The combined extracts were washed with brine, dried with sodium sulfate and concentrated under vacuum give the crude product, which was further purified by silica gel column chromatography (ethyl acetate: petroleum ether = 1: 3) to give target product as a brown solid.

General synthetic procedure 5: deprotection of benzenesulfonyl

A mixture of benzenesulfonyl protected product (1 equiv) and 1 M aqueous sodium hydroxide (5 equiv) in methanol/THF was stirred at room temperature for 10 h. The reaction mixture was concentrated under vacuum and the residue partitioned between saturated sodium bicarbonate solution and DCM. The aqueous phase was extracted twice with DCM. The combined extracts were washed with brine, dried with sodium sulfate, and concentrated under vacuum. Purification by column chromatography on silica gel (DCM: MeOH = 30: 1) afforded target product as a light yellow solid.

General synthetic procedure 6: N alkylation reaction on pyrazole

A solution of bromide (1.5 equiv) in DMF was added to the solution of pyrazole analogues (1.0 equiv) and potassium carbonate (5.0 equiv). The reaction mixture was heated to 80 °C for 4 h. The completion of the reaction was checked with TLC. After cooling to room temperature, water was added and aqueous phase was extracted twice with DCM. The combined extracts were washed with brine, dried with sodium sulfate and concentrated under vacuum give the crude product, which was further purified by silica gel column chromatography (ethyl acetate: petroleum ether = 1: 1) to give target product as a solid.

*4.1.1. Tert-butyl 3-(cyanomethylene) azetidine-1-carboxylate (**11**)*

2-Diethoxyphosphorylacetonitrile (5.7 g, 32.1 mmol) in THF (50 mL) was added to a stirred solution of NaH (1.2 g, 30.7 mmol) in THF (50 mL) at 0 °C. The mixture was stirred at ambient temperature for 1 h then *tert*-butyl 3-oxoazetidine-1-carboxylate (**10**; 5.0 g, 29.2 mmol) in THF was added at 0 °C in 1 h. The mixture was then stirred at ambient temperature for 16 h. The aqueous phase was extracted twice with EA. The combined extracts were washed with brine, dried with sodium sulfate and concentrated under vacuum, the residue was dissolved in CH_3CN (30 mL) and DBU (11.8 g, 77.4 mmol) together with 4-nitropyrazole (3.2g, 28.7 mmol) were added. The mixture was then stirred at ambient temperature for 16 h. Water was added and aqueous phase was extracted twice with EA. The combined extracts were washed with brine, dried with sodium sulfate and concentrated under vacuum give the crude product, which was then dissolved in methanol and purged with argon, palladium on carbon (10% Pd content, 1.4 g, 1.3 mmol) was added, and the reaction mixture stirred under an atmosphere of hydrogen for 12 h. The solids were removed by filtration, washed with methanol and the filtrate concentrated under vacuum to afford 3.5 g (43% for three steps) of **11** as a clear oil.

*4.1.2. 4-Chloro-1-(phenylsulfonyl)-1H-pyrrolo[2,3-b] pyridine (**13**)*

A stirred suspension of 4-chloro-7-azaindole (**12**; 25.0 g, 163.8 mmol) in (DCM) 250 mL was treated with DMAP (2.0 g, 16.5 mmol), triethylamine (34.0 mL, 245.8 mmol), and benzenesulfonyl chloride (23.3 mL, 180.3 mmol) at ambient temperature. The mixture was left to stand overnight. After filtration, the filtrate

was collected and concentrated under vacuum to give a brown solid. Trituration (MeOH) afforded 43.0 g (90%) of **13** as an ashen solid. ^{1}H NMR (300 MHz, $CDCl_3$) δ: 8.36 (d, J = 6.0 Hz, 1H), 8.24 (d, J = 9.0 Hz, 2H), 7.82 (d, J = 6.0 Hz, 1H), 7.64 (t, J = 7.5 Hz, 1H), 7.54 (t, J = 7.5 Hz, 2H), 7.25 (d, J = 6.0 Hz, 1H), 6.76 (d, J = 3.0 Hz, 1H). HRMS (ESI): [M + H] $^+$ calcd for $C_{13}H_{10}ClN_2O_2S$, 293.0146; found, 293.0155.

4.1.3. 4-Chloro-5-nitro-1-(phenylsulfonyl)-1H-pyrrolo[2,3-b] pyridine (**14**)

Tetramethylammonium nitrate (28.0 g, 205.5 mmol) was added to a stirred solution of **3** (30.0 g, 102.7 mmol) in DCM (300 mL) at 25 °C. Trifluoroacetic anhydride (57.3 m0L, 410.8 mmol) was added while maintaining the reaction temperature below 30 °C. The mixture was then stirred at ambient temperature for 5 h. TLC indicated complete reaction. Saturated sodium bicarbonate was added, and the organic phase was separated. The aqueous phase was extracted twice with DCM. The combined extracts were washed with brine, dried with sodium sulfate and concentrated under vacuum to give a yellow solid. Trituration (MeOH) afforded 25.9 g (75%) of **14** as a light yellow solid. ^{1}H NMR (300 MHz, $CDCl_3$) δ: 9.05 (s, 1H), 8.25 (t, J = 4.5 Hz, 2H), 7.99 (d, J = 6.0 Hz, 1H), 7.62–7.57 (m, 3H), 6.92 (d, J = 6.0 Hz, 1H). HRMS (ESI): [M + H] $^+$ calcd for $C_{13}H_9ClN_3O_4S$, 337.9997; found, 338.0010.

4.1.4. Tert-butyl 3-(cyanomethyl)-3-(4-((5-nitro-1-(phenylsulfonyl)-1H-pyrrolo[2,3-b]pyridin-4-yl)amino)-1H-pyrazol-1-yl)azetidine-1-carboxylate (**15**)

A mixture of **14** (3.5 g, 10.5 mmol), **11** (3.5 g, 12.6 mmol), and *N, N*-diisopropylethylamine (5.4 mL, 31.5 mmol) in THF was heated to reflux for 3 h. The cooled reaction mixture was concentrated under vacuum to afford a dark yellow residue. Trituration (MeOH) afforded 4.3 g (70%) of **15** as a yellow solid.

4.1.5. Tert-butyl 3-(4-((5-amino-1-(phenylsulfonyl)-1H-pyrrolo[2,3-b]pyridin-4-yl)amino)-1H-pyrazol-1-yl)-3-(cyanomethyl) azetidine-1-carboxylate (**16**)

A solution of **15** (4.3 g, 7.4 mmol) in methanol was purged with argon, palladium on carbon (10% Pd content, 0.8 g, 0.74 mmol) added, and the reaction mixture stirred under an atmosphere of hydrogen for 12 h. The solids were removed by filtration, washed with methanol and the filtrate concentrated under vacuum to afford 4.0 g (98%) of **16** as a pink powder.

4.1.6. 1H-pyrazol-4-amine (**18**)

A solution of **17** (10.0 g, 88.5 mmol) in methanol was purged with argon, palladium on carbon (10% Pd content, 1.6 g, 1.5 mmol) added, and the reaction mixture stirred under an atmosphere of hydrogen for 12 h. The solids were removed by filtration, washed with methanol and the filtrate concentrated under vacuum to afford 7.3 g (99%) of **18** as a light white powder.

4.1.7. 5-Nitro-1-(phenylsulfonyl)-N-(1H-pyrazol-4-yl)-1H-pyrrolo[2,3-b] pyridin-4-amine (**19**)

A mixture of **14** (23.7 g, 70.3 mmol), **18** (7.0 g, 84.3 mmol), and *N, N*-diisopropylethylamine (24.1 mL, 140.6 mmol) in THF (250 mL) was heated to reflux for 6 h. The cooled reaction mixture was concentrated under vacuum to afford a dark yellow residue. Trituration (MeOH) afforded 18.4 g (68%) of **19** as a dark yellow solid. HRMS (ESI): [M + H] $^+$ calcd for $C_{16}H_{13}N_6O_4S$, 385.0714; found, 385.0668.

4.1.8. 1-(Phenylsulfonyl)-N4-(1H-pyrazol-4-yl)-1H-pyrrolo[2,3-b] pyridine-4,5-diamine (**20**)

A solution of **19** (18.0 g, 46.9 mmol) in methanol was purged with argon, palladium on carbon (10% Pd content, 3.2 g, 3.0 mmol) added, and the reaction mixture stirred under an atmosphere of hydrogen for 12 h. The solids were removed by filtration, washed with methanol and the filtrate concentrated under vacuum to afford 14.9 g (90%) of **20** as a brown powder. HRMS (ESI): [M + H] $^+$ calcd for $C_{16}H_{15}N_6O_2S$, 355.0972; found, 355.0929.

4.1.9. 2-(1-(Ethylsulfonyl)-3-(4-(2-(5-(hydroxymethyl)furan-2-yl) imidazo[4,5-d]pyrrolo[2,3-b]pyridin-1(6H)-yl)-1H-pyrazol-1-yl) azetidin-3-yl)acetonitrile (**1a**)

Synthesized using the **procedure 1, 3, 4 and 5** using 5-hydroxymethylfurfural then ethyl sulfonyl chloride, and 0.2 g (22% for 4 steps) of **1a** was obtained as a light white solid. mp 187–192 °C. ^{1}HNMR(300 MHz, DMSO-d_6): δ = 11.94 (s, 1H), 8.90 (s, 1H), 8.69 (s, 1H), 8.14 (s, 1H), 7.37 (s, 1H), 6.41 (s, 2H), 5.95 (s, 1H), 5.43 (t, J = 6.0 Hz, 1H), 4.62 (d, J = 9.0 Hz, 2H), 4.47 (d, J = 6.0 Hz, 2H), 4.34 (d, J = 9.0 Hz, 2H), 3.78 (s, 2H), 3.32–3.25 (m, 2H), 1.28 (t, J = 7.5 Hz, 4H) ppm; HRMS (ESI): m/z [M+H]$^+$.Calcd for $C_{23}H_{23}N_8O_4S$ 507.1557, found 507.1549.

4.1.10. 2-(1-(Ethylsulfonyl)-3-(4-(2-(5-methylthiophen-2-yl) imidazo[4,5-d]pyrrolo[2,3-b]pyridin-1(6H)-yl)-1H-pyrazol-1-yl) azetidin-3-yl)acetonitrile (**1b**)

Synthesized using the **procedure 1, 3, 4 and 5** using 5-methylthiophene-2-carboxaldehyde then ethyl sulfonyl chloride, and 0.1 (14% for 4 steps) g of **1b** was obtained as a gray solid. mp 191–197 °C. ^{1}HNMR(300 MHz, DMSO-d_6): δ = 11.89 (s, 1H), 8.92 (s, 1H), 8.66 (s, 1H), 8.16 (s, 1H), 7.36 (t, J = 3.0 Hz, 1H), 7.06 (d, J = 3.0 Hz, 1H), 6.78 (d, J = 3.0 Hz, 1H), 5.93–5.91 (m, 1H), 4.61 (d, J = 9.0 Hz, 2H), 4.35 (d, J = 9.0 Hz, 2H), 3.79 (s, 2H), 3.32–3.25 (m, 2H), 2.48 (s, 2H), 1.28 (t, J = 6.0 Hz, 3H) ppm; ^{13}C NMR (75 MHz, DMSO-d_6) δ 146.29, 145.61, 143.37, 139.40, 136.18, 135.26, 133.88, 129.63, 129.13, 128.70, 126.84, 124.77, 119.69, 116.94, 104.54, 96.26, 58.77, 57.28, 43.95, 27.37, 15.24, 7.96 ppm; HRMS (ESI): m/z [M+H]$^+$.Calcd for $C_{23}H_{23}N_8O_2S_2$ 507.1380, found 507.1384.

4.1.11. 2-(1-(Ethylsulfonyl)-3-(4-(2-(thiophen-2-yl)imidazo[4,5-d] pyrrolo[2,3-b]pyridin-1(6H)-yl)-1H-pyrazol-1-yl)azetidin-3-yl) acetonitrile (**1c**)

Synthesized using the **procedure 1, 3, 4 and 5** using 2-thenaldehyde then ethyl sulfonyl chloride, and 0.2 g of **1c** (18% for 4 steps) was obtained as a yellow solid. mp 183–188 °C. ^{1}HNMR(300 MHz, DMSO-d_6): δ = 11.91 (s, 1H), 8.94 (s, 1H), 8.68 (s, 1H), 8.18 (s, 1H), 7.72 (d, J = 6.0 Hz, 1H), 7.36 (t, J = 3.0 Hz, 1H), 7.23 (t, J = 3.0 Hz, 1H), 7.10–7.07 (m, 1H), 5.94–5.92 (m, 2H), 4.61 (d, J = 9.0 Hz, 2H), 4.35 (d, J = 9.0 Hz, 2H), 3.79 (s, 2H), 3.32–3.25 (m, 2H), 1.30–1.25 (m, 4H) ppm; ^{13}C NMR (75 MHz, DMSO-d_6) δ 146.19, 145.64, 139.41, 136.29, 135.39, 133.85, 132.17, 129.61, 129.11, 128.42, 124.80, 119.69, 116.95, 104.56, 58.81, 57.29, 43.93, 27.33, 7.95 ppm; HRMS (ESI): m/z [M+H]$^+$.Calcd for $C_{22}H_{21}N_8O_2S_2$ 493.1223, found 493.1233.

4.1.12. 2-(1-(Ethylsulfonyl)-3-(4-(2-(5-methylfuran-2-yl)imidazo [4,5-d]pyrrolo[2,3-b]pyridin-1(6H)-yl)-1H-pyrazol-1-yl)azetidin-3-yl)acetonitrile (**1d**)

Synthesized using the **procedure 1, 3, 4 and 5** using 5-methyl furfural then ethyl sulfonyl chloride, and 0.2 g of **1d** (11% for 4 steps) was obtained as a light yellow solid. mp 189–193 °C. ^{1}HNMR(300 MHz, DMSO-d_6): δ = 11.91 (s, 1H), 8.89 (s, 1H), 8.67 (s, 1H), 8.13 (s, 1H), 7.37 (t, J = 3.0 Hz, 1H), 6.44 (d, J = 3.0 Hz, 1H), 6.24 (t, J = 3.0 Hz, 1H), 5.95 (t, J = 3.0 Hz, 1H), 4.61 (d, J = 9.0 Hz, 2H), 4.35 (d, J = 9.0 Hz, 2H), 3.78 (s, 2H), 3.33–3.25 (m, 2H), 2.35 (s, 2H), 1.27 (t, J = 4.5 Hz, 5H) ppm; ^{13}C NMR (75 MHz, DMSO-d_6) δ 154.43, 145.72, 143.21, 142.75, 135.76, 135.60, 134.08, 128.65, 124.75, 119.89, 113.60, 108.62, 104.56, 60.25, 58.80, 57.20, 43.90, 26.99, 21.24, 14.55,

13.71, 7.96 ppm; HRMS (ESI): *m/z* [M+H]$^+$.Calcd for $C_{23}H_{23}N_8O_3S$ 491.1608, found 491.1609.

4.1.13. 2-(3-(4-(2-(5-(Hydroxymethyl)furan-2-yl)imidazo[4,5-d]pyrrolo[2,3-b]pyridin-1(6H)-yl)-1H-pyrazol-1-yl)-1-(propylsulfonyl)azetidin-3-yl)acetonitrile (**2a**)

Synthesized using the **procedure 1, 3, 4 and 5** using 5-hydroxymethylfurfural then propyl sulfonyl chloride, and 0.3 g (25% for 4 steps) of **2a** was obtained as a light brown solid. mp 197–202 °C. ^{1}HNMR(300 MHz, DMSO-d_6): δ = 11.91 (s, 1H), 8.87 (s, 1H), 8.66 (s, 1H), 8.11 (s, 1H), 7.34 (s, 1H), 6.38 (s, 2H), 5.93 (s, 1H), 5.40 (t, J = 6.0 Hz, 1H), 4.58 (d, J = 9.0 Hz, 2H), 4.45 (d, J = 3.0 Hz, 2H), 4.31 (d, J = 9.0 Hz, 2H), 3.75 (s, 2H), 3.24 (t, J = 7.5 Hz, 2H), 1.77–1.69 (m, 2H), 1.30–1.18 (m, 2H), 1.00 (t, J = 7.5 Hz, 3H) ppm; ^{13}C NMR (75 MHz, DMSO-d_6) δ 157.85, 145.73, 143.25, 143.07, 139.10, 135.78, 135.68, 134.04, 128.63, 124.75, 119.74, 117.03, 113.11, 109.22, 104.52, 96.44, 58.75, 57.15, 56.11, 50.29, 27.30, 16.89, 13.16 ppm; HRMS (ESI): *m/z* [M+H]$^+$.Calcd for $C_{24}H_{25}N_8O_4S$ 521.1714, found 521.1695.

4.1.14. 2-(1-(Butylsulfonyl)-3-(4-(2-(5-(hydroxymethyl)furan-2-yl)imidazo[4,5-d]pyrrolo[2,3-b]pyridin-1(6H)-yl)-1H-pyrazol-1-yl)azetidin-3-yl)acetonitrile (**3a**)

Synthesized using the **procedure 1, 3, 4 and 5** using 5-hydroxymethylfurfural then butyl sulfonyl chloride, and 0.2 g (27% for 4 steps) of **3a** was obtained as a brown solid. mp 183–187 °C. ^{1}HNMR(300 MHz, DMSO-d_6): δ = 11.95 (s, 1H), 8.90 (s, 1H), 8.69 (s, 1H), 8.14 (s, 1H), 7.37 (s, 1H), 6.41 (s, 2H), 5.96 (s, 1H), 5.44 (t, J = 6.0 Hz, 1H), 4.62 (d, J = 9.0 Hz, 2H), 4.48 (d, J = 6.0 Hz, 2H), 4.35 (d, J = 9.0 Hz, 2H), 3.78 (s, 2H), 3.29 (t, J = 7.5 Hz, 2H), 2.53 (s, 2H), 1.76–1.66 (m, 2H), 1.50–1.38 (m, 2H), 0.92 (t, J = 7.5 Hz, 3H) ppm; ^{13}C NMR (75 MHz, DMSO-d_6) δ 157.86, 145.75, 143.27, 143.09, 139.10, 135.80, 135.69, 134.05, 128.65, 124.76, 119.77, 117.06, 113.13, 109.23, 104.54, 96.46, 58.78, 57.16, 56.13, 48.45, 27.33, 25.08, 21.36, 13.94 ppm; HRMS (ESI): *m/z* [M+H]$^+$.Calcd for $C_{25}H_{27}N_8O_4S$ 535.1870, found 535.1870.

4.1.15. 2-(Thiophen-2-yl)-1-(1-(1-((trifluoromethyl)sulfonyl)azetidin-3-yl)-1H-pyrazol-4-yl)-1,6-dihydroimidazo[4,5-d]pyrrolo[2,3-b]pyridine (**2c**)

Synthesized using the **procedure 1, 6, 3, 4 and 5** using 2-thenaldehyde, 1-Boc-3-iodoazetidine then trifluoromethanesulfonyl chloride, and 0.1 g (9% for 5 steps) of **2c** was obtained as a pink solid. mp 196–201 °C. ^{1}HNMR(300 MHz, DMSO-d_6): δ = 11.93 (s, 1H), 8.68 (s, 1H), 8.62 (s, 1H), 8.17 (s, 1H), 7.73 (d, J = 6.0 Hz, 1H), 7.37 (s, 1H), 7.24 (d, J = 3.0 Hz, 1H), 7.13 (t, J = 4.5 Hz, 1H), 5.89 (s, 1H), 5.65 (s, 1H), 4.87 (t, J = 6.0 Hz, 2H), 4.79 (d, J = 6.0 Hz, 2H) ppm; ^{13}C NMR (75 MHz, DMSO-d_6) δ 146.24, 145.73, 139.58, 136.43, 135.46, 133.93, 132.38, 130.73, 129.66, 128.50, 124.81, 120.51, 118.99, 104.62, 96.52, 64.50, 59.94, 49.83 ppm; HRMS (ESI): *m/z* [M+H]$^+$.Calcd for $C_{19}H_{15}F_3N_7O_2S_2$ 494.0675, found 494.0665.

4.1.16. 1,1,1-Trifluoro-N-(2-(4-(2-(thiophen-2-yl)imidazo[4,5-d]pyrrolo[2,3-b]pyridin-1(6H)-yl)-1H-pyrazol-1-yl)ethyl)methanesulfonamide (**3c**)

Synthesized using the **procedure 1, 6, 4 and 5** using 2-thenaldehyde, 2-bromoethylamine hydrobromide then trifluoromethanesulfonyl chloride, and 0.1 g (17% for 4 steps) of **3c** was obtained as a yellow solid. mp 173–177 °C. ^{1}HNMR(300 MHz, DMSO-d_6): δ = 11.91 (s, 1H), 9.94 (s, 1H), 8.67 (s, 1H), 8.46 (s, 1H), 7.98 (s, 1H), 7.71 (d, J = 6.0 Hz, 1H), 7.34 (t, J = 3.0 Hz, 1H), 7.21 (d, J = 3.0 Hz, 1H), 7.08 (t, J = 4.5 Hz, 1H), 5.95 (s, 1H), 4.49 (t, J = 6.0 Hz, 2H), 3.76 (t, J = 6.0 Hz, 2H) ppm; ^{13}C NMR (75 MHz, DMSO-d_6) δ 146.20, 145.59, 138.17, 136.43, 135.31, 133.84, 132.45, 130.36, 129.39, 128.37, 124.58, 122.32, 120.48, 118.23, 104.62, 96.56, 64.47, 51.96, 44.00 ppm; HRMS (ESI): *m/z* [M+H]$^+$.Calcd for $C_{18}H_{15}F_3N_7O_2S_2$ 482.0675, found 482.0676.

4.1.17. N-(2-(4-(2-(thiophen-2-yl)imidazo[4,5-d]pyrrolo[2,3-b]pyridin-1(6H)-yl)-1H-pyrazol-1-yl)ethyl)propane-1-sulfonamide (**4c**)

Synthesized using the **procedure 1, 6, 4 and 5** using 2-thenaldehyde, 2-bromoethylamine hydrobromide then propyl sulfonyl chloride, and 0.1 g (21% for 4 steps) of **4c** was obtained as a light brown solid. mp 199–204 °C. ^{1}HNMR(300 MHz, DMSO-d_6): δ = 11.90 (s, 1H), 8.66 (s, 1H), 8.42 (s, 1H), 7.94 (s, 1H), 7.71 (d, J = 3.0 Hz, 1H), 7.40 (s, 1H), 7.33 (s, 1H), 7.22 (s, 1H), 7.11 (t, J = 4.5 Hz, 1H), 5.94 (s, 1H), 4.42 (s, 2H), 3.53 (d, J = 6.0 Hz, 2H), 3.08 (t, J = 7.5 Hz, 2H), 1.75–1.67 (m, 2H), 0.99 (t, J = 6.0 Hz, 3H) ppm; ^{13}C NMR (75 MHz, DMSO-d_6) δ 146.23, 145.61, 137.90, 136.44, 135.33, 133.85, 132.43, 130.24, 129.37, 128.46, 124.61, 118.27, 104.63, 96.60, 53.19, 52.43, 42.85, 17.35, 13.14 ppm; HRMS (ESI): *m/z* [M+H]$^+$.Calcd for $C_{20}H_{22}N_7O_2S_2$ 456.1271, found 456.1268.

4.1.18. 2-(1-(Ethylsulfonyl)-3-(4-(imidazo[4,5-d]pyrrolo[2,3-b]pyridin-1(6H)-yl)-1H-pyrazol-1-yl)azetidin-3-yl)acetonitrile (**1e**)

Synthesized using the **procedure 2, 3, 4 and 5** using ethyl sulfonyl chloride, and 0.2 g (33% for 4 steps) of **1e** was obtained as a light white solid. mp 225–230 °C. ^{1}HNMR(300 MHz, DMSO-d_6): δ = 11.96 (s, 1H), 8.87 (s, 1H), 8.70 (s, 1H), 8.36 (s, 1H), 8.21 (s, 1H), 7.43 (t, J = 3.0 Hz, 1H), 6.34 (t, J = 3.0 Hz, 1H), 4.58 (d, J = 9.0 Hz, 2H), 4.32 (d, J = 9.0 Hz, 2H), 3.75 (s, 2H), 3.33–3.26 (m, 2H), 1.29 (t, J = 7.5 Hz, 4H) ppm; ^{13}C NMR (75 MHz, DMSO-d_6) δ 145.62, 142.86, 137.08, 136.05, 135.04, 133.08, 126.19, 124.52, 120.40, 117.12, 104.40, 97.02, 70.39, 64.50, 58.89, 56.94, 43.91, 27.22, 7.92 ppm; HRMS (ESI): *m/z* [M+H]$^+$.Calcd for $C_{18}H_{19}N_8O_2S$ 411.1346, found 411.1351.

4.1.19. 3-(4-(2-(5-(Hydroxymethyl)furan-2-yl)imidazo[4,5-d]pyrrolo[2,3-b]pyridin-1(6H)-yl)-1H-pyrazol-1-yl)propanenitrile (**5a**)

Synthesized using the **procedure 1, 6 and 5** using 5-hydroxymethylfurfural then 3-bromopropionitrile, and 0.2 g (10% for 3 steps) of **5a** was obtained as a light yellow solid. mp 210–215 °C. ^{1}HNMR(300 MHz, DMSO-d_6): δ = 11.89 (s, 1H), 8.66 (s, 1H), 8.50 (s, 1H), 7.96 (s, 1H), 7.35 (t, J = 3.0 Hz, 1H), 6.39 (d, J = 3.0 Hz, 1H), 6.32 (t, J = 3.0 Hz, 1H), 5.96 (t, J = 3.0 Hz, 1H), 5.42 (t, J = 6.0 Hz, 1H), 4.61 (t, J = 6.0 Hz, 2H), 4.48 (d, J = 6.0 Hz, 2H), 3.26 (t, J = 6.0 Hz, 3H) ppm; ^{13}C NMR (75 MHz, DMSO-d_6) δ 157.78, 157.47, 145.67, 143.23, 138.19, 135.90, 135.62, 134.01, 131.03, 127.33, 124.62, 123.63, 119.93, 118.80, 118.63, 104.56, 56.10, 19.18 ppm; HRMS (ESI): *m/z* [M+H]$^+$.Calcd for $C_{19}H_{16}N_7O_2$ 374.1360, found 374.1362.

4.1.20. 2-(4-(2-(5-(Hydroxymethyl)furan-2-yl)imidazo[4,5-d]pyrrolo[2,3-b]pyridin-1(6H)-yl)-1H-pyrazol-1-yl)acetonitrile (**6a**)

Synthesized using the **procedure 1, 6 and 5** using 5-hydroxymethylfurfural then bromoacetonitrile, and 0.1 g (16% for 3 steps) of **6a** was obtained as a dark brown solid. mp 216–219 °C. ^{1}HNMR(300 MHz, DMSO-d_6): δ = 11.89 (s, 1H), 8.67 (d, J = 3.0 Hz, 1H), 8.42 (s, 1H), 7.93 (s, 1H), 7.39 (t, J = 3.0 Hz, 1H), 6.43 (t, J = 3.0 Hz, 1H), 6.35 (d, J = 3.0 Hz, 1H), 6.02 (t, J = 3.0 Hz, 1H), 5.43 (t, J = 6.0 Hz, 1H), 5.33 (s, 1H), 4.49 (d, J = 6.0 Hz, 2H), 3.80 (s, 2H) ppm; ^{13}C NMR (75 MHz, DMSO-d_6) δ 169.13, 157.79, 145.66, 143.25, 138.08, 135.95, 133.97, 131.01, 124.72, 118.97, 112.96, 109.20, 104.62, 96.44, 56.10, 52.96 ppm; HRMS (ESI): *m/z* [M+H]$^+$.Calcd for $C_{18}H_{14}N_7O_2$ 360.1203, found 360.1683.

4.1.21. 3-(4-(2-(5-Methylfuran-2-yl)imidazo[4,5-d]pyrrolo[2,3-b]pyridin-1(6H)-yl)-1H-pyrazol-1-yl)propanenitrile (**5b**)

Synthesized using the **procedure 1, 6 and 5** using 5-methyl

furfural then 3-bromopropionitrile, and 0.1 g (22% for 3 steps) of **5b** was obtained as a yellow solid. mp 215–221 °C. ^{1}HNMR(300 MHz, DMSO-d_6): δ = 11.88 (s, 1H), 8.65 (s, 1H), 8.49 (s, 1H), 7.95 (s, 1H), 7.34 (t, J = 3.0 Hz, 1H), 6.32 (d, J = 6.0 Hz, 1H), 6.21 (t, J = 3.0 Hz, 1H), 5.95 (t, J = 3.0 Hz, 1H), 4.61 (t, J = 6.0 Hz, 2H), 3.26 (t, J = 6.0 Hz, 2H) 2.36 (s, 3H) ppm; ^{13}C NMR (75 MHz, DMSO-d_6) δ 154.37, 145.63, 143.32, 142.66, 138.23, 135.85, 135.51, 134.01, 129.74, 124.61, 118.80, 118.74, 113.49, 108.52, 104.57, 96.45, 48.04, 19.19, 13.71 ppm; HRMS (ESI): m/z [M+H]$^+$.Calcd for $C_{19}H_{16}N_7O$ 358.1411, found 358.1425.

4.1.22. 3-(4-(2-(3-Hydroxyphenyl)imidazo[4,5-d]pyrrolo[2,3-b]pyridin-1(6H)-yl)-1H-pyrazol-1-yl)propanenitrile (*5c*)

Synthesized using the **procedure 1, 6 and 5** using 3-hydroxybenzaldehyde then 3-bromopropionitrile, and 0.2 g (16% for 3 steps) of **5c** was obtained as a gray solid. mp 247–250 °C. ^{1}HNMR(300 MHz, DMSO-d_6): δ = 11.87 (s, 1H), 9.66 (s, 1H), 8.69 (s, 1H), 8.41 (s, 1H), 7.86 (s, 1H), 7.34 (t, J = 3.0 Hz, 1H), 7.26 (t, J = 3.0 Hz, 1H), 7.19 (t, J = 9.0 Hz, 1H), 7.07 (t, J = 3.0 Hz, 1H), 6.87–6.83 (m, 1H), 6.00 (t, J = 3.0 Hz, 1H), 4.56 (t, J = 6.0 Hz, 2H), 3.21 (t, J = 6.0 Hz, 2H) ppm; ^{13}C NMR (75 MHz, DMSO-d_6) δ 157.65, 150.93, 145.56, 138.25, 136.49, 135.68, 133.84, 131.18, 129.86, 129.55, 124.45, 119.89, 119.64, 118.73, 117.04, 116.29, 104.76, 96.65, 47.97, 19.17 ppm; HRMS (ESI): m/z [M+H]$^+$.Calcd for $C_{20}H_{16}N_7O$ 370.1411, found 370.1425.

4.1.23. 3-(4-(2-(5-Methylthiophen-2-yl)imidazo[4,5-d]pyrrolo[2,3-b]pyridin-1(6H)-yl)-1H-pyrazol-1-yl)propanenitrile (*5d*)

Synthesized using the **procedure 1, 6 and 5** using 5-methylthiophene-2-carboxaldehyde then 3-bromopropionitrile, and 0.1 g (17% for 3 steps) of **5d** was obtained as a light yellow solid. mp 210–216 °C. ^{1}HNMR(300 MHz, DMSO-d_6): δ = 11.86 (s, 1H), 8.64 (s, 1H), 8.52 (s, 1H), 7.98 (s, 1H), 7.33 (t, J = 3.0 Hz, 1H), 7.03 (d, J = 3.0 Hz, 1H), 6.78 (d, J = 3.0 Hz, 1H), 5.92 (t, J = 3.0 Hz, 1H), 4.62 (d, J = 6.0 Hz, 2H), 3.27 (d, J = 6.0 Hz, 2H), 2.47 (s, 3H) ppm; ^{13}C NMR (75 MHz, DMSO-d_6) δ 146.32, 145.59, 143.22, 138.52, 136.31, 135.24, 133.88, 130.18, 129.84, 128.52, 126.81, 124.60, 118.77, 118.67, 104.58, 96.35, 48.09, 19.26, 15.27 ppm; HRMS (ESI): m/z [M+H]$^+$.Calcd for $C_{19}H_{16}N_7S$ 374.1182, found 374.1195.

4.1.24. 3-(4-(2-(2-Chlorophenyl)imidazo[4,5-d]pyrrolo[2,3-b]pyridin-1(6H)-yl)-1H-pyrazol-1-yl)propanenitrile (*5e*)

Synthesized using the **procedure 1, 6 and 5** using 2-chlorobenzaldehyde then 3-bromopropionitrile, and 0.1 g (21% for 3 steps) of **5e** was obtained as a light green solid. mp 186–191 °C. ^{1}HNMR(300 MHz, DMSO-d_6): δ = 11.93 (s, 1H), 8.72 (s, 1H), 8.29 (s, 1H), 7.70 (d, J = 9.0 Hz, 2H), 7.55 (t, J = 3.0 Hz, 2H), 7.44–7.52 (m, 1H), 7.39 (t, J = 3.0 Hz, 1H), 6.16 (t, J = 3.0 Hz, 1H), 4.46 (t, J = 6.0 Hz, 2H) 3.12 (t, J = 6.0 Hz, 2H) ppm; ^{13}C NMR (75 MHz, DMSO-d_6) δ 149.44, 145.60, 137.55, 135.83, 134.93, 134.02, 133.74, 133.22, 132.17, 129.88, 129.80, 128.90, 127.47, 124.63, 118.62, 118.27, 104.56, 96.73, 47.82, 19.04 ppm; HRMS (ESI): m/z [M+H]$^+$.Calcd for C_{20}-$H_{15}ClN_7$ 388.1072, found 388.1102.

4.1.25. 3-(4-(2-(4-(Methylsulfonyl)phenyl)imidazo[4,5-d]pyrrolo[2,3-b]pyridin-1(6H)-yl)-1H-pyrazol-1-yl)propanenitrile (*5f*)

Synthesized using the **procedure 1, 6 and 5** using 4-methylsulphonyl benzaldehyde then 3-bromopropionitrile, and 0.1 g (31% for 3 steps) of **5f** was obtained as a dark yellow solid. mp 198–203 °C. ^{1}HNMR(300 MHz, DMSO-d_6): δ = 11.97 (s, 1H), 8.77 (s, 1H), 8.49 (s, 1H), 8.03–7.96 (m, 4H), 7.92 (s, 1H), 7.39 (t, J = 3.0 Hz, 1H), 6.04 (d, J = 3.0 Hz, 1H), 4.59 (t, J = 7.5 Hz, 2H), 3.28 (s, 3H), 3.23 (t, J = 7.5 Hz, 2H) ppm; ^{13}C NMR (75 MHz, DMSO-d_6) δ 149.14, 145.68, 141.54, 138.28, 136.68, 136.08, 134.74, 134.00, 129.95, 129.86, 127.54, 124.72, 119.15, 118.75, 104.68, 96.79, 48.03, 43.79, 19.29 ppm; HRMS (ESI): m/z [M+H]$^+$.Calcd for $C_{21}H_{18}N_7O_2S$ 432.1237, found 432.1241.

4.1.26. 3-(4-(2-(Trifluoromethyl)imidazo[4,5-d]pyrrolo[2,3-b]pyridin-1(6H)-yl)-1H-pyrazol-1-yl)propanenitrile (*5g*)

Synthesized using the **procedure 1, 6 and 5** using trifluoroacetaldehyde then 3-bromopropionitrile, and 0.2 g (33% for 3 steps) of **5g** was obtained as a white solid. mp 218–222 °C. ^{1}HNMR(300 MHz, DMSO-d_6): δ = 12.18 (s, 1H), 8.84 (s, 1H), 8.56 (s, 1H), 8.04 (s, 1H), 7.45 (t, J = 3.0 Hz, 1H), 6.05 (d, J = 3.0 Hz, 1H), 4.61 (t, J = 6.0 Hz, 2H), 3.25 (t, J = 6.0 Hz, 2H) ppm; ^{13}C NMR (75 MHz, DMSO-d_6) δ 146.31, 139.10, 138.59, 138.09, 137.05, 136.31, 132.02, 129.84, 125.29, 120.89, 118.68, 117.30, 116.51, 104.31, 97.01, 48.05, 19.10 ppm; HRMS (ESI): m/z [M+H]$^+$.Calcd for $C_{15}H_{11}F_3N_7$ 346.1023, found 346.1049.

4.1.27. 3-(4-(2-(Thiophen-2-yl)imidazo[4,5-d]pyrrolo[2,3-b]pyridin-1(6H)-yl)-1H-pyrazol-1-yl)propanenitrile (*5h*)

Synthesized using the **procedure 1, 6 and 5** using 2-thenaldehyde then 3-bromopropionitrile, and 0.2 g (22% for 3 steps) of **5h** was obtained as a light yellow solid. mp 221–226 °C. ^{1}HNMR(300 MHz, DMSO-d_6): δ = 11.94 (s, 1H), 8.69 (s, 1H), 8.57 (s, 1H), 8.04 (s, 1H), 7.74 (d, J = 6.0 Hz, 1H), 7.37 (t, J = 3.0 Hz, 1H), 7.22 (d, J = 3.0 Hz, 1H), 7.10 (t, J = 4.5 Hz, 1H), 5.96 (d, J = 3.0 Hz, 1H), 4.65 (t, J = 6.0 Hz, 2H), 3.30 (t, J = 6.0 Hz, 2H) ppm; ^{13}C NMR (75 MHz, DMSO-d_6) δ 146.22, 145.67, 138.58, 136.44, 135.42, 133.90, 132.46, 130.23, 129.51, 128.30, 124.67, 120.51, 118.75, 104.62, 96.43, 64.50, 48.12, 19.29 ppm; HRMS (ESI): m/z [M+H]$^+$.Calcd for $C_{18}H_{14}N_7S$ 360.1026, found 360.1033.

4.1.28. 3-(4-(2-(Thiazol-2-yl)imidazo[4,5-d]pyrrolo[2,3-b]pyridin-1(6H)-yl)-1H-pyrazol-1-yl)propanenitrile (*5i*)

Synthesized using the **procedure 1, 6 and 5** using 2-thiazolecarboxaldehyde then 3-bromopropionitrile, and 0.2 g (31% for 3 steps) of **5i** was obtained as a yellow solid. mp 247–250 °C. ^{1}HNMR(300 MHz, DMSO-d_6): δ = 12.04 (s, 1H), 8.76 (s, 1H), 8.44 (s, 1H), 7.95–7.91 (m, 3H), 7.38 (t, J = 3.0 Hz, 1H), 6.04 (t, J = 3.0 Hz, 1H), 4.59 (t, J = 6.0 Hz, 2H), 3.25 (t, J = 6.0 Hz, 2H) ppm; ^{13}C NMR (75 MHz, DMSO-d_6) δ 157.89, 145.93, 144.50, 138.49, 136.63, 136.15, 135.26, 133.75, 132.31, 129.71, 124.78, 123.35, 120.51, 118.88, 114.62, 104.62, 97.09, 70.39, 64.50, 61.55, 52.70, 49.75, 47.93, 19.20 ppm; HRMS (ESI): m/z [M+H]$^+$.Calcd for $C_{17}H_{13}N_8S$ 361.0978, found 361.2340.

4.1.29. 3-(4-(2-(Thiazol-5-yl)imidazo[4,5-d]pyrrolo[2,3-b]pyridin-1(6H)-yl)-1H-pyrazol-1-yl)propanenitrile (*5j*)

Synthesized using the **procedure 1, 6 and 5** using thiazole-5-carboxaldehyde then 3-bromopropionitrile, and 0.2 g (19% for 3 steps) of **5j** was obtained as a dark yellow solid. mp 227–231 °C. ^{1}HNMR(300 MHz, DMSO-d_6): δ = 11.98 (s, 1H), 9.20 (s, 1H), 8.70 (s, 1H), 8.56 (s, 1H), 8.01 (d, J = 6.0 Hz, 2H), 7.37 (t, J = 3.0 Hz, 1H), 5.97 (d, J = 3.0 Hz, 1H), 4.64 (t, J = 6.0 Hz, 2H), 3.27 (t, J = 6.0 Hz, 2H) ppm; ^{13}C NMR (75 MHz, DMSO-d_6) δ 156.69, 145.70, 144.30, 143.13, 138.53, 136.36, 135.59, 134.08, 130.36, 128.12, 124.81, 118.82, 118.08, 104.55, 96.50, 48.18, 19.26 ppm; HRMS (ESI): m/z [M+H]$^+$.Calcd for $C_{17}H_{13}N_8S$ 361.0978, found 361.2341.

4.1.30. 3-(4-(Imidazo[4,5-d]pyrrolo[2,3-b]pyridin-1(6H)-yl)-1H-pyrazol-1-yl)propanenitrile (*5k*)

Synthesized using the **procedure 2, 6 and 5** using 3-bromopropionitrile, and 0.1 g (15% for 3 steps) of **5k** was obtained as a light white solid. mp 258–262 °C. ^{1}HNMR(300 MHz, DMSO-d_6): δ = 11.94 (s, 1H), 8.68 (s, 1H), 8.51 (s, 1H), 8.32 (s, 1H), 8.04 (s, 1H), 7.42 (t, J = 3.0 Hz, 1H), 6.36 (t, J = 4.5 Hz, 1H), 4.58 (t, J = 6.0 Hz, 2H), 3.23 (t, J = 6.0 Hz, 2H) ppm; ^{13}C NMR (75 MHz, DMSO-d_6) δ 157.67, 150.90, 145.57, 138.27, 136.51, 135.69, 133.84,

131.18, 129.89, 129.57, 124.49, 119.93, 119.65, 118.74, 117.08, 116.31, 104.78, 96.67, 47.98, 19.18 ppm; HRMS (ESI): *m/z* $[M+H]^+$.Calcd for $C_{14}H_{12}N_7$ 278.1149, found 278.1955.

4.1.31. 4-(4-(Imidazo[4,5-d]pyrrolo[2,3-b]pyridin-1(6H)-yl)-1H-pyrazol-1-yl)butanenitrile (**6k**)

Synthesized using the **procedure 2, 6 and 5** using 4-bromobutyronitrile, and 0.1 g (31% for 3 steps) of **6k** was obtained as a white solid. mp 197–200 °C. ^{1}HNMR(300 MHz, DMSO-d_6): δ = 11.91 (s, 1H), 8.67 (s, 1H), 8.44 (s, 1H), 8.28 (s, 1H), 7.98 (s, 1H), 7.42 (t, *J* = 3.0 Hz, 1H), 6.31 (d, *J* = 3.0 Hz, 1H), 4.37 (t, *J* = 7.5 Hz, 2H), 2.62 (t, *J* = 7.5 Hz, 2H), 2.27–2.18 (m, 2H) ppm; ^{13}C NMR (75 MHz, DMSO-d_6) δ 145.58, 142.92, 136.06, 135.56, 135.11, 133.05, 127.12, 124.43, 120.47, 119.25, 104.45, 96.98, 51.09, 26.24, 14.35 ppm; HRMS (ESI): *m/z* $[M+H]^+$.Calcd for $C_{15}H_{14}N_7$ 292.1305, found 292.1314.

4.1.32. 5-(4-(Imidazo[4,5-d]pyrrolo[2,3-b]pyridin-1(6H)-yl)-1H-pyrazol-1-yl)pentanenitrile (**7k**)

Synthesized using the **procedure 2, 6 and 5** using 5-bromovaleronitrile, and 0.1 g (13% for 3 steps) of **7k** was obtained as a gray solid. mp 203–207 °C. ^{1}HNMR(300 MHz, DMSO-d_6): δ = 11.91 (s, 1H), 8.68 (s, 1H), 8.43 (s, 1H), 8.31 (s, 1H), 7.97 (s, 1H), 7.42 (t, *J* = 3.0 Hz, 1H), 6.26 (d, *J* = 3.0 Hz, 1H), 4.33 (t, *J* = 7.5 Hz, 2H), 2.63 (t, *J* = 7.5 Hz, 2H), 2.05–1.95 (m, 2H), 1.68–1.58 (m, 2H) ppm; ^{13}C NMR (75 MHz, DMSO-d_6) δ 145.55, 142.94, 136.06, 135.40, 135.09, 133.14, 127.01, 124.42, 120.98, 118.98, 104.45, 96.80, 51.50, 29.32, 22.51, 16.21 ppm; HRMS (ESI): *m/z* $[M+H]^+$.Calcd for $C_{16}H_{16}N_7$ 306.1462, found 306.1468.

4.1.33. 1-(1-(4,4,4-Trifluorobutyl)-1H-pyrazol-4-yl)-1,6-dihydroimidazo[4,5-d]pyrrolo[2,3-b]pyridine (**8k**)

Synthesized using the **procedure 2, 6 and 5** using 1-bromo-4,4,4-trifluorobutane, and 0.1 g (16% for 3 steps) of **8k** was obtained as a light yellow solid. mp 176–179 °C. ^{1}HNMR(300 MHz, DMSO-d_6): δ = 11.96 (s, 1H), 8.68 (s, 1H), 8.46 (s, 1H), 8.32 (s, 1H), 7.99 (s, 1H), 7.43 (t, *J* = 3.0 Hz, 1H), 6.26 (t, *J* = 3.0 Hz, 1H), 4.38 (t, *J* = 6.0 Hz, 2H), 2.44–2.30 (m, 2H), 2.19–2.10 (m, 2H) ppm; ^{13}C NMR (75 MHz, DMSO-d_6) δ 145.67, 143.09, 136.17, 135.75, 135.23, 133.22, 132.31, 129.89, 127.30, 124.56, 123.46, 120.51, 119.24, 114.62, 107.14, 104.55, 96.86, 70.39, 64.50, 61.55, 52.70, 51.09, 49.75, 30.50, 23.26 ppm; HRMS (ESI): *m/z* $[M+H]^+$.Calcd for $C_{15}H_{14}F_3N_6$ 335.1227, found 335.2531.

4.1.34. 4-(4-(2-(5-Methylfuran-2-yl)imidazo[4,5-d]pyrrolo[2,3-b]pyridin-1(6H)-yl)-1H-pyrazol-1-yl)butanenitrile (**6b**)

Synthesized using the **procedure 1, 6 and 5** using 5-methyl furfural then 4-bromobutyronitrile, and 0.2 g (21% for 3 steps) of **6b** was obtained as a white solid. mp 201–206 °C. ^{1}HNMR(300 MHz, DMSO-d_6): δ = 11.93 (s, 1H), 8.66 (s, 1H), 8.44 (s, 1H), 7.93 (s, 1H), 7.38 (s, 1H), 6.35 (d, *J* = 6.0 Hz, 1H), 6.26 (d, *J* = 3.0 Hz, 1H), 5.88 (s, 1H), 4.41 (t, *J* = 6.0 Hz, 2H), 2.64 (t, *J* = 6.0 Hz, 2H), 2.31 (s, 3H), 2.28–2.22 (m, 2H) ppm; ^{13}C NMR (75 MHz, DMSO-d_6) δ 154.23, 145.67, 143.30, 142.83, 137.64, 135.86, 135.58, 134.07, 129.42, 124.66, 120.37, 118.74, 113.43, 108.56, 104.59, 96.30, 51.14, 26.31, 14.29, 13.73 ppm; HRMS (ESI): *m/z* $[M+H]^+$.Calcd for $C_{20}H_{18}N_7O$ 372.1567, found 372.2493.

4.1.35. 4-(4-(2-(2-Aminothiazol-5-yl)imidazo[4,5-d]pyrrolo[2,3-b]pyridin-1(6H)-yl)-1H-pyrazol-1-yl)butanenitrile (**7b**)

Synthesized using the **procedure 1, 6 and 5** using 2-aminothiazole-5-carboxaldehyde then 4-bromobutyronitrile, and 0.2 g (19% for 3 steps) of **7b** was obtained as a dark brown solid. mp 219–225 °C. ^{1}HNMR(300 MHz, DMSO-d_6): δ = 11.84 (s, 1H), 8.58 (s, 1H), 8.45 (s, 1H), 7.96 (s, 1H), 7.53 (s, 1H), 7.34 (s, 1H), 7.00 (s, 1H), 5.81 (s, 1H), 4.41 (s, 2H), 2.63 (d, *J* = 9.0 Hz, 2H), 2.26 (t, *J* = 6.0 Hz, 2H) ppm; ^{13}C NMR (75 MHz, DMSO-d_6) δ 170.74, 145.80, 145.53, 140.56, 137.94, 136.13, 134.81, 134.12, 129.80, 124.62, 120.35, 118.56, 114.53, 104.51, 96.01, 51.18, 26.33, 14.28 ppm; HRMS (ESI): *m/z* $[M+H]^+$.Calcd for $C_{18}H_{16}N_9S$ 390.1244, found 390.2187.

4.1.36. 4-(4-(2-(5-Methylthiophen-2-yl)imidazo[4,5-d]pyrrolo[2,3-b]pyridin-1(6H)-yl)-1H-pyrazol-1-yl)butanenitrile (**6d**)

Synthesized using the **procedure 1, 6 and 5** using 5-methylthiophene-2-carboxaldehyde then 4-bromobutyronitrile, and 0.2 g (24% for 3 steps) of **6d** was obtained as a yellow solid. mp 221–227 °C. ^{1}HNMR(300 MHz, DMSO-d_6): δ = 11.90 (s, 1H), 8.65 (s, 1H), 8.46 (s, 1H), 7.96 (s, 1H), 7.36 (t, *J* = 3.0 Hz, 1H), 7.06 (d, *J* = 6.0 Hz, 1H), 6.82 (t, *J* = 3.0 Hz, 1H), 5.84 (t, *J* = 3.0 Hz, 1H), 4.41 (t, *J* = 7.5 Hz, 2H), 2.63 (t, *J* = 7.5 Hz, 2H), 2.48 (s, 3H), 2.31–2.21 (m, 2H) ppm; ^{13}C NMR (75 MHz, DMSO-d_6) δ 146.34, 145.62, 143.14, 137.98, 136.33, 135.31, 133.93, 129.70, 128.60, 126.77, 124.66, 120.34, 118.66, 104.62, 96.17, 60.22, 51.20, 26.34, 21.19, 15.26, 14.52, 14.26 ppm; HRMS (ESI): *m/z* $[M+H]^+$.Calcd for $C_{20}H_{18}N_7S$ 388.1339, found 388.2289.

4.1.37. 2-(5-Methylthiophen-2-yl)-1-(1-(4,4,4-trifluorobutyl)-1H-pyrazol-4-yl)-1,6-dihydroimidazo[4,5-d]pyrrolo[2,3-b]pyridine (**7d**)

Synthesized using the **procedure 1, 6 and 5** using 5-methylthiophene-2-carboxaldehyde then 1-bromo-4,4,4-trifluorobutane, and 0.2 g (26% for 3 steps) of **7d** was obtained as a yellow solid. mp 199–206 °C. ^{1}HNMR(300 MHz, DMSO-d_6): δ = 11.90 (s, 1H), 8.64 (s, 1H), 8.45 (s, 1H), 7.96 (s, 1H), 7.35 (t, *J* = 3.0 Hz, 1H), 7.09 (d, *J* = 3.0 Hz, 1H), 6.81 (d, *J* = 3.0 Hz, 1H), 5.80 (d, *J* = 3.0 Hz, 1H), 4.42 (t, *J* = 7.5 Hz, 2H), 2.46 (s, 3H), 2.40–2.27 (m, 2H), 2.20–2.10 (m, 2H) ppm; ^{13}C NMR (75 MHz, DMSO-d_6) δ 146.36, 145.60, 143.16, 138.06, 136.32, 135.33, 133.94, 129.95, 129.78, 128.59, 126.63, 126.04, 124.62, 118.55, 104.60, 95.97, 51.10, 30.57, 30.19, 23.29, 15.17 ppm; HRMS (ESI): *m/z* $[M+H]^+$.Calcd for $C_{20}H_{18}F_3N_6S$ 431.1260, found 431.2250.

4.1.38. 5-(4-(2-(5-Methylthiophen-2-yl)imidazo[4,5-d]pyrrolo[2,3-b]pyridin-1(6H)-yl)-1H-pyrazol-1-yl)pentanenitrile (**8d**)

Synthesized using the **procedure 1, 6 and 5** using 5-methylthiophene-2-carboxaldehyde then 5-bromovaleronitrile, and 0.2 g (31% for 3 steps) of **8d** was obtained as a yellow solid. mp 208–214 °C. ^{1}HNMR(300 MHz, DMSO-d_6): δ = 11.91 (s, 1H), 8.64 (s, 1H), 8.43 (s, 1H), 7.94 (s, 1H), 7.35 (t, *J* = 3.0 Hz, 1H), 7.05 (d, *J* = 6.0 Hz, 1H), 6.83 (d, *J* = 3.0 Hz, 1H), 5.81 (d, *J* = 3.0 Hz, 1H), 4.37 (t, *J* = 6.0 Hz, 2H), 2.65 (t, *J* = 7.5 Hz, 2H), 2.48 (s, 3H), 2.06–1.97 (m, 2H), 1.68–1.59 (m, 2H) ppm; ^{13}C NMR (75 MHz, DMSO-d_6) δ 146.36, 145.60, 143.21, 137.81, 136.38, 135.32, 133.93, 129.88, 129.78, 128.50, 126.76, 124.70, 120.98, 118.37, 104.62, 96.05, 51.65, 29.42, 22.52, 16.21, 15.32 ppm; HRMS (ESI): *m/z* $[M+H]^+$.Calcd for $C_{21}H_{20}N_7S$ 402.1495, found 402.2456.

4.1.39. 4-(4-(2-Methylimidazo[4,5-d]pyrrolo[2,3-b]pyridin-1(6H)-yl)-1H-pyrazol-1-yl)butanenitrile (**9a**)

Synthesized using the **procedure 1, 6 and 5** using acetaldehyde then 4-bromobutyronitrile, and 0.2 g (18% for 3 steps) of **9a** was obtained as a white solid. mp 197–203 °C. ^{1}HNMR(300 MHz, DMSO-d_6): δ = 11.81 (s, 1H), 8.54 (s, 1H), 8.40 (s, 1H), 7.93 (s, 1H), 7.35 (t, *J* = 3.0 Hz, 1H), 6.02 (t, *J* = 3.0 Hz, 1H), 4.38 (t, *J* = 7.5 Hz, 2H), 2.62 (t, *J* = 7.5 Hz, 2H), 2.51 (s, 3H), 2.28–2.19 (m, 2H) ppm; ^{13}C NMR (75 MHz, DMSO-d_6) δ 150.67, 145.39, 136.87, 134.86, 133.71, 128.49, 124.30, 120.37, 118.49, 104.50, 96.15, 51.14, 26.18, 14.33, 14.09 ppm; HRMS (ESI): *m/z* $[M+H]^+$.Calcd for $C_{16}H_{16}N_7$ 306.1462, found 306.1478.

4.1.40. 4-(4-(2-Cyclopropylimidazo[4,5-d]pyrrolo[2,3-b]pyridin-1(6H)-yl)-1H-pyrazol-1-yl)butanenitrile (**9b**)

Synthesized using the **procedure 1, 6 and 5** using cyclopropanecarboxaldehyde then 4-bromobutyronitrile, and 0.2 g (34% for 3 steps) of **9b** was obtained as a white solid. mp 205–209 °C. ^{1}HNMR(300 MHz, DMSO-d_6): δ = 11.71 (s, 1H), 8.43 (s, 1H), 8.37 (s, 1H), 7.88 (s, 1H), 7.28 (d, J = 3.0 Hz, 1H), 5.94 (d, J = 3.0 Hz, 1H), 4.32 (t, J = 6.0 Hz, 2H), 2.55 (t, J = 7.5 Hz, 2H), 2.22–2.13 (m, 2H), 1.98–1.91 (m, 1H), 1.03–0.98 (m, 4H) ppm; ^{13}C NMR (75 MHz, DMSO-d_6) δ 155.63, 145.32, 137.16, 135.03, 134.77, 133.48, 128.80, 124.31, 120.38, 118.20, 104.46, 96.15, 51.15, 26.21, 14.34, 9.27, 7.85 ppm; HRMS (ESI): m/z [M+H]$^+$.Calcd for $C_{18}H_{18}N_7$ 332.1618, found 332.1610.

4.1.41. 4-(4-(2-Cyclobutylimidazo[4,5-d]pyrrolo[2,3-b]pyridin-1(6H)-yl)-1H-pyrazol-1-yl)butanenitrile (**9c**)

Synthesized using the **procedure 1, 6 and 5** using cyclobutanecarboxaldehyde then 4-bromobutyronitrile, and 0.2 g (27% for 3 steps) of **9c** was obtained as a light yellow solid. mp 211–217 °C. ^{1}HNMR(300 MHz, DMSO-d_6): δ = 11.80 (s, 1H), 8.60 (s, 1H), 8.33 (s, 1H), 7.85 (s, 1H), 7.33 (t, J = 3.0 Hz, 1H), 5.95 (t, J = 3.0 Hz, 1H), 4.37 (t, J = 6.0 Hz, 2H), 3.75–3.64 (m, 1H), 2.63–2.53 (m, 2H), 2.52–2.43 (m, 2H), 2.27–2.18 (m, 4H), 2.06–1.83 (m, 2H) ppm; ^{13}C NMR (75 MHz, DMSO-d_6) δ 156.70, 145.42, 137.05, 135.20, 133.71, 128.65, 124.28, 120.35, 118.20, 104.57, 96.18, 51.12, 32.02, 27.56, 26.24, 18.45, 14.32 ppm; HRMS (ESI): m/z [M+H]$^+$.Calcd for $C_{19}H_{20}N_7$ 346.1775, found 346.1805.

4.1.42. 4-(4-(2-Cyclopentylimidazo[4,5-d]pyrrolo[2,3-b]pyridin-1(6H)-yl)-1H-pyrazol-1-yl)butanenitrile (**9d**)

Synthesized using the **procedure 1, 6 and 5** using cyclopentanecarbaldehyde then 4-bromobutyronitrile, and 0.2 g (29% for 3 steps) of **9d** was obtained as a light yellow solid. mp 227–232 °C. ^{1}HNMR(300 MHz, DMSO-d_6): δ = 11.81 (s, 1H), 8.56 (s, 1H), 8.41 (s, 1H), 7.90 (s, 1H), 7.32 (s, 1H), 5.89 (s, 1H), 4.38 (t, J = 6.0 Hz, 2H), 3.31–3.18 (m, 1H), 2.62 (t, J = 6.0 Hz, 2H), 2.26 (t, J = 6.0 Hz, 2H), 1.94 (t, J = 6.0 Hz, 4H), 1.78 (s, 2H), 1.62 (d, J = 6.0 Hz, 2H) ppm; ^{13}C NMR (75 MHz, DMSO-d_6) δ 157.87, 145.32, 137.40, 135.34, 135.02, 133.49, 129.04, 124.28, 120.36, 118.30, 104.55, 96.03, 51.11, 36.62, 32.29, 26.20, 25.81, 14.28 ppm; HRMS (ESI): m/z [M+H]$^+$.Calcd for $C_{20}H_{22}N_7$ 360.1931, found 360.1935.

4.2. Biologic assays

4.2.1. Enzyme assay

Recombinant kinases of human JAK enzymes were purchased from Carna Biosciences Inc. (JAK1: 08–144; JAK2: 08–045; JAK3: 08–046; TYK2: 08–147), and Kinase substrate22, 30 and Kinase JAK1 peptide were from GL Inc. (Kinase substrate22: 112393; Kinase substrate30: 117885; Kinase JAK1 peptide: 758318). The 250 nL samples of test compounds and controls solubilized in 100% DMSO were added to a 384-well polypropylene plate using a noncontact acoustic dispenser. Kinase assays were carried out at room temperature in a 15 μL reaction buffer containing 20 mM HEPES, pH 7.4, 1 mM ATP, 10 mM magnesium chloride, 0.01% bovine serum albumin (BSA), 0.0005% Tween 20, and 1 mM DTT. The assays were initiated by the addition of enzyme. The assays were stopped with 30 μL of a buffer containing 180 mM HEPES, pH 7.4, 20 mM EDTA, 0.2% Coating Reagent, resulting in a final concentration of 10 mM EDTA, 0.1% Coating Reagent, and 100 mM HEPES, pH 7.4. The conversion% were read by Caliper EZ Reader.

4.2.2. Cellular assays

The activities of compounds were determined in cell-based assays that are designed to measure JAK-dependent STAT phosphorylation. TF-1 cells are cultured in RPMI 1640 + 10% FBS+2 ng/mL Recombinant Human Protein GM-CSF medium. Cells are maintained in log phase before the assay. Compounds were serially diluted in DMSO and incubated for 2 h at 37 °C with TF-1 cells in 384-well microtiter plates in RPMI-1640 at a final cell density of 40,000 cells per well. freshly prepared GM-CSF (final conc. 100 ng/ml) were then added at the final concentrations indicated to the microtiter plates containing the TF-1 cells and compounds and the plates were incubated for 10 min at 37 °C. Cells are lysed by adding 4 μl lysis buffer and shaking for 30 min at room temperature. Add 4 μL/well of premixed antibody solutions prepared in the detection buffer. Cover the plate with a plate sealer. Incubate overnight at room temperature. Read plate (HTRF protocol) on Envision (plate reader). THP-1 cells are cultured in RPMI 1640 + 10% FBS+0.05 mM 2-mercaptoethanol medium. Cells are maintained in log phase before the assay. Cell pellets are collected and re-suspended in serum free and phenol free RPMI1640 medium. 40,000 cells/well (10 μl) are seeded in each well of 384-well plate. Compounds were serially diluted in DMSO and incubated for 2 h at 37 °C with THP-1 cells. Stimulate cells with freshly prepared IL-4 (final conc. 200 ng/ml), incubate for 10 min at 37 °C. Cells are lysed by adding 4 μl lysis buffer and shaking for 30 min at room temperature. Add 4 μL/well of premixed antibody solutions prepared in the detection buffer. Cover the plate with a plate sealer. Incubate overnight at room temperature. Read plate (HTRF protocol) on Envision (plate reader).

4.2.3. Microsomal metabolism

The liver is the main organ of drug metabolism in the body. Subcellular fractions such as liver microsomes are useful in vitro models of hepatic clearance as they contain many of the drug metabolising enzymes found in the liver. Microsomes are easy to prepare and can be stored for long periods of time. They are easily adaptable to high throughput screens which enable large numbers of compounds to be screened rapidly and inexpensively. The metabolic stability is conducted in microsomes at time-gradient (5, 10, 20, 30, 60, 120 min). Microsomes (0.8 mg/mL) are incubated with the test compounds (1 μM) at 37 °C in the presence of the cofactor, NADPH, which initiates the reaction. After the incubation period, the reaction is terminated by the addition of Acetonitrile. Following centrifugation, the amount of parent compound in the supernatant is quantified by HPLC-MS/MS. The percentage of metabolism is calculated by comparing the peak area of the parent compound versus zero time point control.

4.2.4. JAK2-STAT pathway assay

TF-1 cells were cultured in RPMI-1640 with 10% FBS + 2 ng/ml GM-CSF and incubated at 37 °C in a 5% CO_2 incubator. TF-1 cells were plated at density of 6×10^6 cells/well in a 6-well plate. After 24 h cultivation, the cells were treated with different concentrations of compounds and further cultured for 3 h. Then, cells were collected and lysed. Proteins were resolved by SDS-polyacrylamide gel electrophoresis, transferred to a PVDF membrane. Membrane was blocked in 5% non-fat dried milk in Tris-buffered saline (pH7.4) containing 0.1% Tween 20 (TBST) for 0.5 h and subsequently incubated with primary antibodies diluted in TBST at 4 °C overnight. Membranes were then probed with horseradish Peroxidase-conjugated secondary antibodies and developed using enhanced chemiluminescence (ECL) reagent. Band intensities were measured using ImageJ software program. The antibodies used in these experiments are pSTAT5 (Y694), β-actin antibodies.

4.2.5. Pharmacokinetic in rats

The pharmacokinetics of test compounds were evaluated following intravenous injection (IV) or oral administration (PO) of

solution at doses of 1–20 mg/kg in Lewis rats. Compounds were dissolved in 70/20/10 Normal Saline/PEG400/DMSO. Blood samples for IV or PO dose groups were collected prior to administration (Predose) and at 0.03, 0.08, 0.17, 0.33, 0.5, 1, 2, 4, 6, 8, 12 and 24 h post dose. The vehicle used for IV and PO dose groups was a combination of PEG400 with citrate buffer (pH5.0) or PEG400 with DMSO/Normal Saline. Plasma concentrations were quantitated using a non-validated LC/MS/MS method. PK parameters were determined by non-compartmental methods using WinNonlin (version 8.0).

4.2.6. Pharmacodynamics in mice

C57 mice were orally administered Normal Saline, or ascending doses (10–50 mg/kg) of compound **6k** formulated in DMSO/PEG400/Normal Saline = 10:20:70 in 200 μL volume at t = 0. 30 min later, mice were stimulated intraperitoneally with 1 μg recombinant mouse GM-CSF in 10 μL saline. 30 min after GM-CSF administration, animals were sacrificed and snap frozen spleen samples were collected for analysis of concentrations of pSTAT3 and pSTAT5, respectively. Spleen homogenates were thawed on ice, and their total protein concentration was measured by the ELISA method (Jianglai Biological Technology Co. LTD; JL13517, JL50768) per the manufacturer's protocol.

Declaration of competing interest

The authors declare that they have no known competing financial interests or personal relationships that could have appeared to influence the work reported in this paper.

Acknowledgments

We gratefully acknowledge financial support for the National Natural Science Foundation of China (no. 21672260), the financial support of the National Natural Science Foundation of Jiangsu Province of China (no. BK20170743 and BK20171393), a National Innovation and Entrepreneurship Training Program For College Students (201910316030S) the 'Double FirstClass' University Project (CPU2018GY07), and the State Key Laboratory of Drug Research (SIMM1903KF-03) and Postgraduate Research & Practice Innovation Program of Jiangsu Province (KYCX18_0770).

Appendix A. Supplementary data

Supplementary data to this article can be found online at https://doi.org/10.1016/j.ejmech.2021.113394.

References

[1] A.A. Daniel, O. Attilio, H. Robert, T. Jürgen, J.B. Michael, M. Le, B. Michelle, D.B. Clara, C. Mario, W.V. James, The 2016 revision to the World Health Organization classification of myeloid neoplasms and acute leukemia, Blood 127 (2016) 2391–2406, https://doi.org/10.1515/jtim-2017-0002.

[2] R.D. Legare, D.G. Gilliland, Myelodysplastic syndrome, Curr. Opin. Hematol. 2 (1995) 283–292, https://doi.org/10.1097/00062752-199502040-00008.

[3] V. Monali, R. Syed, L. Xin, E.V. Kent, Z. Hong, Novel immunotherapies for hematological malignancies, Curr. Mol. Pharmacol. 9 (2016) 264–271, https://doi.org/10.2174/1874467208666150716121253.

[4] S. Vesna, T. Natasa, K. Tatjana, P. Sonja, C. Milica, JAK2-V617F mutation in patients with myeloproliferative neoplasms: association with FLT3-ITD mutation, Srp. Arh. Celok. Lek. 138 (2010) 614–618, https://doi.org/10.2298/SARH1010614S.

[5] W.L. Emily, M.S. Susan, Ruxolitinib: a new treatment for myelofibrosis, Clin. J. Oncol. Nurs. 17 (2013) 312–318, https://doi.org/10.1188/13.CJON.312-318.

[6] A.D. William, A.C.-H. Lee, S. Blanchard, A. Poulsen, E.L. Teo, H. Nagaraj, E. Tan, D. Chen, M. Williams, E.T. Sun, K.C. Goh, W.C. Ong, S.K. Goh, S. Hart, R. Jayaraman, M.K. Pasha, K. Ethirajulu, J.M. Wood, B.W. Dymock, Discovery of the macrocycle 11-(2-pyrrolidin-1-yl-ethoxy)-14, 19-dioxa-5,7,26-triaza-tetracyclo[19.3.1.1(2,6).1(8,12)]heptacosa-1(25),2(26),3,5,8,10,12(27),16,21,23-decaene (SB1518), a potent janus kinase 2/fms-like tyrosine kinase-3 (JAK2/FLT3) inhibitor for the treatment of myelofibrosis and lymphoma, J. Med. Chem. 54 (2011) 4638–4658, https://doi.org/10.1021/jm200326p.

[7] H. Yu, D. Pardoll, R. Jove, STATs in cancer inflammation and immunity: a leading role for STAT3, Nat. Rev. Canc. 9 (2009) 798–809, https://doi.org/10.1038/nrc2734.

[8] J. Lim, B. Taoka, R.D. Otte, K. Spencer, C.J. Dinsmore, M.D. Altman, G. Chan, C. Rosenstein, S. Sharma, H.P. Su, A.A. Szewczak, L. Xu, H. Yin, J. Zugay-Murphy, C.G. Marshall, J.R. Young, Discovery of 1-amino-5H-pyrido[4,3-b]indol-4-carboxamide inhibitors of janus kinase 2 (JAK2) for the treatment of myeloproliferative disorders, J. Med. Chem. 54 (2011) 7334–7349, https://doi.org/10.1021/jm200909u.

[9] F. Perner, C. Perner, T. Ernst, F.H. Heidel, Roles of JAK2 in aging, inflammation, hematopoiesis and malignant transformation, Cells 8 (2019) 854–872, https://doi.org/10.3390/cells8080854.

[10] J. Mascarenhas, R. Hoffman, Ruxolitinib: the first FDA approved therapy for the treatment of myelofibrosis, Clin. Canc. Res. 18 (2012) 3008–3014, https://doi.org/10.1158/1078-0432.CCR-11-3145.

[11] A.B. Hannah, Fedratinib: first approval, Drugs 79 (2019) 1719–1725, https://doi.org/10.1007/s40265-019-01205-x.

[12] H. Wan, G.M. Schroeder, A.C. Hart, J. Inghrim, J. Grebinski, J.S. Tokarski, M.V. Lorenzi, D. You, T. Mcdevitt, B. Penhallow, R. Vuppugalla, Y. Zhang, X. Gu, R. Iyer, L.J. Lombardo, G.L. Trainor, S. Ruepp, J. Lippy, Y. Blat, J.S. Sack, J.A. Khan, K. Stefanski, B. Sleczka, A. Mathur, J. Sun, M.K. Wong, D. Wu, P. Li, A. Gupta, P.N. Arunachalam, B. Pragalathan, S. Narayanan, K.C. Nanjundaswamy, P. Kuppusamy, A.V. Purandare, Discovery of a highly selective JAK2 inhibitor, BMS-911543, for the treatment of myeloproliferative neoplasms, ACS Med. Chem. Lett. 6 (2015) 850–855, https://doi.org/10.1021/acsmedchemlett.5b00226.

[13] A.C. Hart, G.M. Schroeder, H. Wan, J. Grebinski, J. Inghrim, J. Kempson, J. Guo, W.J. Pitts, J.S. Tokarski, J.S. Sack, J.A. Khan, J. Lippy, M.V. Lorenzi, D. You, T. McDevitt, R. Vuppugalla, Y. Zhang, L.J. Lombardo, G.L. Trainor, A.V. Purandare, Structure-Based design of selective janus kinase 2 imidazo[4,5-d]pyrrolo[2,3-b]pyridine inhibitors, ACS Med. Chem. Lett. 6 (2015) 845–849, https://doi.org/10.1021/acsmedchemlett.5b00225.

[14] M. Zak, C.A. Hurley, S.I. Ward, P. Bergeron, K. Barrett, M. Balazs, W.S. Blair, R. Bull, P. Chakravarty, C. Chang, P. Crackett, G. Deshmukh, J. DeVoss, P.S. Dragovich, C. Eigenbrot, C. Ellwood, S. Gaines, N. Ghilardi, P. Gibbons, S. Gradl, P. Gribling, C. Hamman, E. Harstad, P. Hewitt, A. Johnson, T. Johnson, J.R. Kenny, M.F.T. Koehler, P. Bir Kohli, S. Labadie, W.P. Lee, J. Liao, M. Liimatta, R. Mendonca, R. Narukulla, R. Pulk, A. Reeve, S. Savage, S. Shia, M. Steffek, S. Ubhayakar, A. van Abbema, I. Aliagas, B. Avitabile-Woo, Y. Xiao, J. Yang, J.J. Kulagowski, Identification of C-2 hydroxyethyl imidazopyrrolopyridines as potent JAK1 inhibitors with favorable physicochemical properties and high selectivity over JAK2, J. Med. Chem. 56 (2013) 4764–4785, https://doi.org/10.1021/jm4004895.

[15] D.C. James, E.F. Mark, T. Jean-Baptiste, Discovery and development of janus kinase (JAK) inhibitors for inflammatory diseases, J. Med. Chem. 57 (2014) 5023–5038, https://doi.org/10.1021/jm401490p.

[16] S. Ioannidis, M.L. Lamb, T. Wang, L. Almeida, M.H. Block, A.M. Davies, B. Peng, M. Su, H. Zhang, E. Hoffmann, C. Rivard, I. Green, T. Howard, H. Pollard, J. Read, M. Alimzhanov, G. Bebernitz, K. Bell, M. Ye, D. Huszar, M. Zinda, Discovery of 5-chloro-N2-[(1S)-1-(5-fluoropyrimidin-2-yl) ethyl]-N4-(5-methyl-1H-pyrazol-3-yl) pyrimidine-2,4-diamine (Azd1480) as a novel inhibitor of the jak/stat pathway, J. Med. Chem. 54 (2011) 262–276, https://doi.org/10.1021/jm1011319.

[17] V. Swapna, R. Raphaël, R. Stephanie, S.D. Girdhar, F. Lori, T. Arthur, J. Amy, S. Melissa, K. Albane, E. Amanda, T.C. Artur, S. Julian, R. Ana, M.A. Vicky, J.P. Matthew, B.B. Jonathan, Discovery of potent N-ethylurea pyrazole derivatives as dual inhibitors of trypanosoma brucei and trypanosoma cruzi, ACS Med. Chem. Lett. 11 (2020) 278–285, https://doi.org/10.1021/acsmedchemlett.9b00218.

[18] M. Zak, R. Mendonca, M. Balazs, K. Barrett, P. Bergeron, W.S. Blair, C. Chang, G. Deshmukh, J. DeVoss, P.S. Dragovich, C. Eigenbrot, N. Ghilardi, P. Gibbons, S. Gradl, C. Hamman, E.J. Hanan, E. Harstad, P.R. Hewitt, C.A. Hurley, T. Jin, A. Johnson, T. Johnson, J.R. Kenny, M.F.T. Koehler, P. Bir Kohli, J.J. Kulagowski, S. Labadie, J. Liao, M. Liimatta, Z. Lin, P.J. Lupardus, R.J. Maxey, J.M. Murray, R. Pulk, M. Rodriguez, S. Savage, S. Shia, M. Steffek, S. Ubhayakar, M. Ultsch, A. van Abbema, S.I. Ward, L. Xiao, Y. Xiao, Discovery and optimization of C-2 methyl imidazopyrrolopyridines as potent and orally bioavailable JAK1 inhibitors with selectivity over JAK2, J. Med. Chem. 55 (2012) 6176–6193, https://doi.org/10.1021/jm300628c.

[19] J.J. Kulagowski, W. Blair, R.J. Bull, C. Chang, G. Deshmukh, H.J. Dyke, C. Eigenbrot, N. Ghilardi, P. Gibbons, T.K. Harrison, P.R. Hewitt, M. Liimatta, C.A. Hurley, A. Johnson, T. Johnson, J.R. Kenny, P. Bir Kohli, R.J. Maxey, R. Mendonca, K. Mortara, J. Murray, R. Narukulla, S. Shia, M. Steffek, S. Ubhayakar, M. Ultsch, A. van Abbema, S.I. Ward, B. Waszkowycz, M. Zak, Identification of imidazo-pyrrolopyridines as novel and potent JAK1 inhibitors, J. Med. Chem. 55 (2012) 5901–5921, https://doi.org/10.1021/jm300438j.

[20] M.K. Kim, H. Shin, K. Park, H. Kim, J. Park, K. Kim, J. Nam, H. Choo, Y. Chong, Benzimidazole derivatives as potent JAK1-selective inhibitors, J. Med. Chem. 58 (2015) 7596–7602, https://doi.org/10.1021/acs.jmedchem.5b01263.

[21] A. Ritzen, M.D. Sørensen, K.N. Dack, D.R. Greve, A. Jerre, M.A. Carnerup, K.A. Rytved, J. Bagger-Bahnsen, Fragment-Based discovery of 6-arylindazole JAK inhibitors, ACS Med. Chem. Lett. 7 (2016) 641–646, https://doi.org/

10.1021/acsmedchemlett.6b00087.
[22] E.G. Yang, N. Mustafa, E.C. Tan, A. Poulsen, P.M. Ramanujulu, W.J. Chong, J.J.Y. Yen, B.W. Dymock, Design and synthesis of janus kinase 2 (JAK2) and histone deacetlyase (HDAC) bispecific inhibitors based on pacritinib and evidence of dual pathway inhibition in hematological cell lines, J. Med. Chem. 59 (2016) 8233–8262, https://doi.org/10.1021/acs.jmedchem.6b00157.
[23] B. Shubhasree, B. Ann, G. Massimo, H. Sarfaraz, M.S. Daniella, JAK–STAT signaling as a target for inflammatory and autoimmune diseases: current and future prospects, Drugs 77 (2017) 521–546, https://doi.org/10.1007/s40265-017-0736-y.